

CONFIDENTIAL

NASA TM X-183

NASA TM X-183

NASA

Classification changed to declassify
effective 1 April 1983 under
Authority of NASA OGC 2 by
Carroll.

N63-13897
Code-1

TECHNICAL MEMORANDUM

X-183

USE OF EXPERIMENTAL STEADY-FLOW AERODYNAMIC PARAMETERS
IN THE CALCULATION OF FLUTTER CHARACTERISTICS FOR
FINITE-SPAN SWEPT OR UNSWEPT WINGS AT
SUBSONIC, TRANSONIC, AND

SUPERSONIC SPEEDS

By E. Carson Yates, Jr.

Langley Research Center
Langley Field, Va.

CLASSIFIED DOCUMENT - TITLE UNCLASSIFIED

This material contains information affecting the national defense of the United States within the meaning of the espionage laws, Title 18, U.S.C., Secs. 793 and 794, the transmission or revelation of which in any manner to an unauthorized person is prohibited by law.

NATIONAL AERONAUTICS AND SPACE ADMINISTRATION
WASHINGTON

January 1960

CONFIDENTIAL

03171289J040

Code-1

Copy # 1

03171289J040

CONFIDENTIAL

NATIONAL AERONAUTICS AND SPACE ADMINISTRATION

TECHNICAL MEMORANDUM X-183

USE OF EXPERIMENTAL STEADY-FLOW AERODYNAMIC PARAMETERS

IN THE CALCULATION OF FLUTTER CHARACTERISTICS FOR

FINITE-SPAN SWEPT OR UNSWEPT WINGS AT

SUBSONIC, TRANSONIC, AND

SUPERSONIC SPEEDS*

By E. Carson Yates, Jr.

SUMMARY

Flutter calculations for several swept and unswept wings through the transonic speed range have been made by the modified strip-theory method of NACA RM L57L10, which employs steady-flow aerodynamic parameters for the undeformed wing. Experimentally determined distributions of steady-flow aerodynamic parameters for the undeformed wings were used in the present calculations. Comparisons of these calculated results with experimental flutter data and with calculations previously made by using linearized-theory aerodynamic parameters indicate that the method employed gives accurate flutter results for swept wings at subsonic, transonic, and supersonic speeds. However, since this method of flutter calculation is not applicable when the Mach number component normal to the leading edge is near 1.0, it appears that the transonic flutter characteristics of unswept wings cannot be calculated by the method as given in NACA RM L57L10. An attempt was made to remove this limitation by using experimental values of two-dimensional lift-curve slope (instead of theoretical values) in the calculation of circulation functions when the Mach number component normal to the leading edge was near 1.0. Applying this procedure to two unswept wings removed the spurious asymptotic rise of flutter speed near Mach number 1.0, but it did not result in very close agreement between calculated and experimental flutter speeds.

The possibility of obtaining estimates of flutter characteristics for unswept wings by use of total aerodynamic parameters has also been examined. Although no supersonic calculations were made using total aerodynamic parameters, it appears that the procedure outlined gives reasonable estimates of flutter characteristics at subsonic speeds.

*Title, Unclassified.

CONFIDENTIAL

INTRODUCTION

Reference 1 presented a strip-theory type of flutter calculation procedure for finite-span swept and unswept wings based on spanwise distributions of lift and pitching moment derived from distributions of aerodynamic parameters associated with the undeformed wing in steady flow.¹ Subsonic and supersonic flutter characteristics for several wings were calculated by this modal analysis method and compared with experimental flutter data. However, all the calculated results shown in reference 1 were obtained by the use of steady-flow aerodynamic parameters calculated from linearized theory, and hence no calculations were shown for Mach numbers near 1.0. Since minimum flutter speeds usually occur for Mach numbers near 1.0, it was not possible to evaluate the minimum flutter speed by using these theoretical steady-flow aerodynamic parameters.

Some linearized-theory methods exist for calculating three-dimensional oscillating aerodynamic loads at sonic speed (for example, ref. 2). However, the application of such calculations to finite-thickness wings which involve mixed-flow regions is open to question. The reliability of these methods has not been proved in actual use.

The present report presents the results of flutter calculation for several wings through the transonic range, made by the method of reference 1, but employing experimentally determined distributions of steady-flow aerodynamic parameters obtained from wind-tunnel and flight tests. It may be noted that use of experimental steady-flow aerodynamic parameters introduces into the flutter calculation some nonlinear aerodynamic effects such as those of finite thickness and viscosity. The magnitudes of these steady-flow nonlinear effects are believed to be approximately correct for the oscillating wing as long as the frequency is not too high.

The possibility of obtaining estimates of flutter characteristics for unswept wings by use of experimental total aerodynamic parameters is also examined herein.

In the discussion of the limitations of the flutter calculation procedure in reference 1, it was pointed out that because a two-dimensional lift-curve slope appeared in the expressions for the circulation functions used, the method as presented was not applicable when the Mach number

¹In the method of reference 1 spanwise distributions of steady-flow section lift-curve slope and local aerodynamic center for the undeformed wing are used in conjunction with the "effective" angle-of-attack distribution resulting from the assumed vibration modes in order to obtain values of section lift and pitching moment. Circulation functions modified on the basis of loadings for two-dimensional airfoils oscillating in compressible flow are employed to account for the effects of oscillatory motion on the magnitudes and phase angles of the lift and moment vectors.

CONFIDENTIAL

CONFIDENTIAL

3

component normal to the wing leading edge was very close to 1.0. (The theoretical two-dimensional lift-curve slope, employed in the calculation of circulation functions in reference 1, approaches infinity as the Mach number component normal to the wing leading edge approaches 1.0.) The possibility of removing this limitation by using experimental values of two-dimensional lift-curve slope in the circulation functions is examined in the present report.

Flutter characteristics calculated by using experimentally determined distributions of static aerodynamic parameters are herein compared with experimental flutter data, and with the flutter characteristics calculated for the same wings in reference 1 from the theoretical distributions of static aerodynamic parameters. Uncoupled vibration modes are employed in all flutter calculations. Calculations are shown for three swept wings of aspect ratio 4.0, taper ratio 0.6, quarter-chord sweep angle 45° , and local center-of-gravity positions at approximately 34 percent chord, 46 percent chord, and 58 percent chord. Calculations are shown for two unswept wings of aspect ratio 4.0, taper ratio 0.6, quarter-chord sweep angle 0, and local center-of-gravity positions at approximately 45 percent chord and 59 percent chord. Finally, some flutter characteristics calculated by using experimentally determined total static aerodynamic parameters are shown for the two unswept wings mentioned previously and for a wing of aspect ratio 4.0, taper ratio 1.0, sweep angle 0, and local center of gravity at 50 percent chord.

SYMBOLS

A	aspect ratio of full wing including fuselage intercept
a	nondimensional distance from midchord to elastic axis measured perpendicular to elastic axis, positive rearward, fraction of semichord b
ac	nondimensional distance from leading edge to local aerodynamic center (for steady flow) measured streamwise, fraction of streamwise chord
ac _n	nondimensional distance from midchord to local aerodynamic center (for steady flow) measured perpendicular to elastic axis, positive rearward, fraction of semichord b, see equation (2)
ac _N	value obtained by applying equation (2) to total ac value for the wing. Total ac is defined as the nondimensional distance from leading edge of mean aerodynamic chord to wing aerodynamic-center position (for steady flow) measured streamwise, fraction of mean aerodynamic chord.

CONFIDENTIAL

CONFIDENTIAL

4

CONFIDENTIAL

b	semichord of wing measured perpendicular to elastic axis
b_r	semichord of wing measured perpendicular to elastic axis at spanwise reference station $\eta = 0.75$
C	complex circulation function, $F + iG$
C_{l_α}	local lift-curve slope for a streamwise section in steady flow
$C_{l_{\alpha,n}}$	local lift-curve slope for a section perpendicular to elastic axis in steady flow
C_{L_α}	total lift-curve slope for wing in steady flow
F	real part of complex circulation function C
G	imaginary part of complex circulation function C
k_{nr}	reduced frequency based on spanwise reference station ($\eta = 0.75$) and on velocity component normal to elastic axis, $\frac{b_r \omega}{V \cos \Lambda_{ea}}$
M	stream Mach number
M_{LE}	Mach number component normal to the leading edge
V	flutter speed, measured parallel to free stream (experimental values or values calculated by the method of ref. 1)
V_R	calculated reference flutter speed obtained by using $C_{l_{\alpha,n}} = 2\pi \cdot ac_n = -\frac{1}{2}$, and $C = F_I + iG_I$
β_{LE}	$\sqrt{ M_{LE}^2 - 1 }$
Λ	sweep angle, positive for sweepback
λ	taper ratio of full wing including fuselage intercept
η	nondimensional coordinate (either spanwise or along elastic axis) measured from wing root, fraction of exposed panel span or fraction of wing length
ρ	air density

CONFIDENTIAL

ω circular frequency of vibration

ω_α circular frequency of first uncoupled torsional vibration
mode of wing measured about elastic axis

Subscripts:

$c/4$ quantities associated with wing quarter chord

$c/2$ quantities associated with wing midchord

$.4c$ quantities associated with wing 40 percent chord

ea quantities associated with wing elastic axis

C circulation functions obtained from oscillatory aerodynamic
coefficients for a two-dimensional wing in compressible flow

I circulation functions for two-dimensional incompressible flow

PROCEDURE FOR USING EXPERIMENTAL STEADY-FLOW AERODYNAMIC
PARAMETERS IN THE FLUTTER CALCULATIONS

Since the experimental steady-flow aerodynamic parameters used herein were obtained from several sources, and since these parameters are applied to several wings, table I has been prepared as a guide to the flutter calculations presented in this report.

Spanwise Distributions of Lift-Curve Slope
and Aerodynamic Center

Wings with 45° sweepback.- Experimental spanwise distributions of steady-flow lift-curve slope C_{l_α} and aerodynamic center ac for the plan form of $A = 4.0$, $\lambda = 0.6$, $\Lambda_{c/4} = 45^\circ$ were obtained from the data of references 3 and 4 over the Mach number range from 0.6 to 1.2. It should be noted that the wing of references 3 and 4 was 6 percent thick (NACA 65A006 airfoil) while the experimental flutter data of references 5 and 6 with which calculated flutter characteristics are to be compared, were obtained with wings that were 4 percent thick (NACA 65A004 airfoil). No correction has been applied to the steady-flow aerodynamic parameters to account for this difference of thickness.

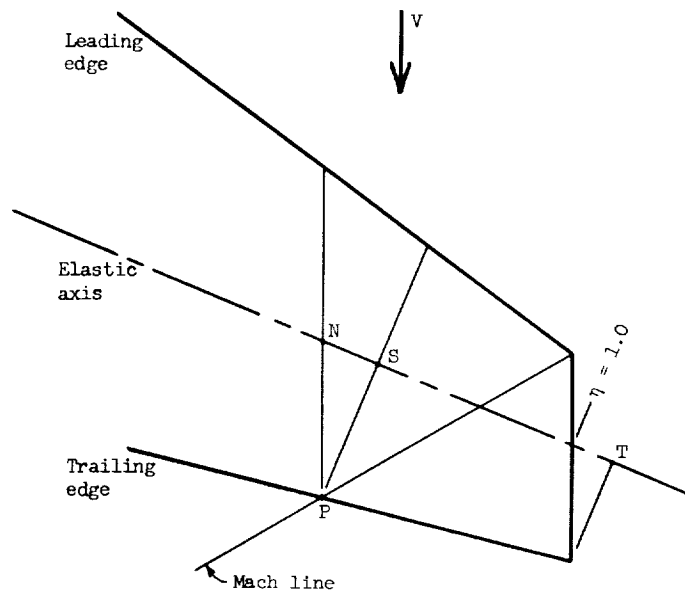
Since the modified strip analysis of reference 1 utilizes aerodynamic and structural quantities associated with wing strips normal to the wing elastic axis, equations (B6) and (B7) of reference 1 were used to convert C_{l_α} and a_c (associated with the streamwise direction) to $C_{l_{\alpha,n}}$ and a_{c_n} (associated with the direction normal to the elastic axis). (See solid curves of figs. 1 and 2.) For convenience, these geometrical relations are repeated here in the notation of the present report:

$$C_{l_{\alpha,n}} = \frac{C_{l_\alpha}}{\cos \Lambda_{ea}} \quad (1)$$

$$a_{c_n} = \left(2a_c \left\{ \cos \Lambda_{ea} + \left[\tan \Lambda_c/4 - \frac{1}{A} \frac{1-\lambda}{1+\lambda} (1-2a) \right] \sin \Lambda_{ea} \right\} - (1+a) \left[\cos \Lambda_{ea} + \left(\tan \Lambda_c/4 + \frac{1}{A} \frac{1-\lambda}{1+\lambda} \right) \sin \Lambda_{ea} \right] \right) \cos \Lambda_{ea} + a \quad (2)$$

Crossplots of these values of $C_{l_{\alpha,n}}$ and a_{c_n} against stream Mach number M for several spanwise stations are shown in figure 3.

Direct application of equations (1) and (2) for supersonic speeds immediately raises a question with regard to the η station at which the tip begins to affect $C_{l_{\alpha,n}}$ and a_{c_n} . As shown in the accompanying sketch,



a consideration only of strips normal to the elastic axis, indicates that the tip influences strips only outboard of point S. However, the experimental distributions of $C_{l_{\alpha}}$ and ac obtained from the data of references 3 and 4 are associated with the streamwise direction, and hence the tip affects all strips outboard of point N. In order to adapt the streamwise data near the tip to the strip orientation employed in the flutter calculation, the $C_{l_{\alpha,n}}$ and ac_n distributions obtained from equations (1) and (2) were cut at station N, and the portions outboard of that point were affinely compressed into the η range outboard of point S by the relation

$$1 - \eta_{\text{corrected}} = (1 - \eta) \frac{1 - \eta_S}{1 - \eta_N} \quad (\eta_N \leq \eta \leq 1) \quad (3)$$

The $C_{l_{\alpha,n}}$ and ac_n values inboard of point N were, of course, left unchanged. In the gap thus created between points N and S the $C_{l_{\alpha,n}}$ and ac_n curves were closed by a faired line which as nearly as possible represented an extension of the inboard values. Thus tip effects are confined to wing sections outboard of point S, and the faired loading between sections N and S logically represents a continuation of the inboard loading and is unaffected by the tip. Values of $C_{l_{\alpha,n}}$ and ac_n obtained in this manner are given by the dashed curves of figs. 1 and 2. Figures 1 and 2 indicate that compared to values of $C_{l_{\alpha,n}}$ and ac_n obtained directly from equations (1) and (2), the result of the above alteration is to increase the lift-curve slope and to move the aerodynamic center rearward in the tip region. These changes will in general oppose each other in their effect on the calculated flutter speed. For supersonic Mach numbers flutter calculations have been made both with the $C_{l_{\alpha,n}}$ and ac_n values obtained directly from equations (1) and (2) (solid curves of figs. 1 and 2) and with $C_{l_{\alpha,n}}$ and ac_n values altered as described above (dashed curves of figs. 1 and 2).

From the preceding sketch it also appears that a strict integration of lifting pressure in the direction normal to the elastic axis will yield finite loads as far outboard as point T. However, in accordance with the strip-analysis method of reference 1, no loads are considered outboard of $\eta = 1.0$.

The wing of references 3 and 4 was statically tested in the presence of a fuselage with maximum radius equal to 13.9 percent of the wing semi-span. The flutter data with which the calculated flutter characteristics for the 45° wings are to be compared (refs. 5 and 6) were obtained in the

presence of a fuselage with radius equal to 21.9 percent of the wing semispan. Therefore, only the values of $C_{l_{\alpha,n}}$ and ac_n outboard of the 21.9-percent-semispan station were used in the flutter calculations. That is, $\eta = 0$ corresponds to 21.9-percent semispan. The effects of the different fuselage sizes on the distributions of $C_{l_{\alpha,n}}$ and ac_n are generally confined to the neighborhood of the wing root. Such effects should therefore have negligible influence on the calculated flutter characteristics.

Unswep wings with taper ratio of 0.6. Experimental spanwise distributions of steady-flow lift-curve slope $C_{l_{\alpha}}$ and aerodynamic center ac for the plan form of $A = 4.0$, $\lambda = 0.6$, $\Lambda_{c/4} = 0$ were obtained from the data of reference 7 over the Mach number range from 0.6 to 1.05 and from unpublished flight test data for the X-1E airplane at $M = 1.41$. The wing of reference 7 had $A = 4.0$, $\lambda = 0.5$, $\Lambda_{c/2} = 0$, and hence had a plan form which was slightly different from that of the flutter-tested wings (ref. 5). However, the wing of reference 7 as well as the flutter-tested wings had NACA 65A004 airfoil sections. The wing of the X-1E airplane had $A = 4.0$, $\lambda = 0.5$, $\Lambda_{c/4} = 0$, and a modified NACA 64A004 airfoil, and thus also differed slightly in plan form and airfoil from the flutter-tested wings. No correction was applied to the steady-flow aerodynamic parameters to account for these small differences, and the distributions of $C_{l_{\alpha,n}}$ and ac_n obtained from the data of reference 7 and from the unpublished data for the X-1E airplane were used directly in the flutter calculations.

For the unswept wings the effect of the wing tip on the steady-flow aerodynamic parameters for each wing strip is properly accounted for without application of a tip correction of the type previously discussed for swept wings. For unswept wings the freestream direction and the direction normal to the elastic axis essentially coincide so that

$$C_{l_{\alpha,n}} = C_{l_{\alpha}}$$

and

$$ac_n = 2ac - 1$$

The wing of reference 7 was statically tested in the presence of a fuselage with maximum radius equal to 12.35 percent of the wing semispan, and the maximum fuselage radius of the X-1E airplane was 20.5 percent of

the wing semispan. The flutter-test wings of reference 5 were tested in the presence of a fuselage with radius equal to 21.9 percent of wing semispan. The treatment of these different fuselage sizes is the same as that described previously for the 45° swept wings.

The spanwise distributions of $C_{l_{\alpha,n}}$ and ac_n obtained from the data of reference 7 are shown in figure 4. Crossplots of these values of $C_{l_{\alpha,n}}$ and ac_n against stream Mach number for three spanwise stations are shown in figure 5. Spanwise distributions of $C_{l_{\alpha,n}}$ and ac_n obtained from flight-test data for the X-1E airplane at $M = 1.41$ are shown in figure 6 and are compared with values from reference 1 calculated from linearized supersonic-flow theory.

Total Lift-Curve Slope and Aerodynamic

Center for Unswept Wings

The feasibility of using experimental total lift-curve slope $C_{L_{\alpha}}$ and aerodynamic center ac_N in flutter calculations has been investigated for three unswept wings. It has been observed for a number of unswept wings that the spanwise distribution of $C_{l_{\alpha}}/C_{L_{\alpha}}$ does not vary greatly as stream Mach number M increases from subsonic to transonic to low supersonic. Furthermore, the spanwise distributions of experimental $C_{l_{\alpha}}/C_{L_{\alpha}}$ have been found to be close to those calculated by the method of reference 8. Therefore, the total lift-curve slope $C_{L_{\alpha}}$ is introduced into the flutter calculation as a multiplying factor applied to the calculated spanwise distribution of $C_{l_{\alpha}}/C_{L_{\alpha}}$ obtained from the method of reference 8 for $M = 0.75$. Thus

$$C_{l_{\alpha}} = \left(C_{L_{\alpha}} \right)_{M, \text{exp}} \times \left(\frac{C_{l_{\alpha}}}{C_{L_{\alpha}}} \right)_{M = 0.75, \text{calc}} \quad (4)$$

In the absence of a reliable method for estimating spanwise distribution of aerodynamic center at transonic speeds it is assumed in all flutter calculations involving total aerodynamic parameters that ac is constant across the span and that

$$ac = ac_{\text{total}} \quad (5)$$

where ac_{total} is referred to the mean aerodynamic chord. Although equation (5) may be reasonably valid for unswept wings at subsonic speeds, it is realized that equation (5) is not a good approximation to the loading characteristics of a wing at transonic and supersonic speeds. It does, however, permit the introduction of the qualitative variation of aerodynamic center with Mach number. The appropriateness of equation (5) will, of course, be determined by the results obtained by using it.

Unswept wings with taper ratio of 0.6.- For the plan form of $A = 4.0$, $\lambda = 0.6$, $\Lambda_c/4 = 0$, experimental values of C_{L_α} and ac_N in the Mach number range from 0.6 to 1.15 were obtained from the data of reference 9. These values are shown in figure 7 together with the spanwise distribution of C_{l_α} for $M = 0.75$ calculated by the method of reference 8.

Unswept wings with taper ratio of 1.0.- For the wing of $A = 4.0$, $\lambda = 1.0$, $\Lambda_c/4 = 0$, experimental values of C_{L_α} and ac_N were obtained from reference 10 in the Mach number range from 0.6 to 1.10 and from reference 11 in the Mach number range from 0.4 to 1.05. The wing of reference 10 had an NACA 65A004 airfoil, and that of reference 11 had an NACA 63A004 airfoil. The wing for which the flutter-test data were given in reference 12 had a 4-percent-thick hexagonal airfoil. The C_{L_α} and ac_N values obtained from the data of references 10 and 11 are shown in figure 8 together with the spanwise distribution of C_{l_α} for $M = 0.75$ calculated by the method of reference 8.

Use of Experimental Two-Dimensional Lift-Curve Slope in the Calculation of Circulation Functions

In the flutter calculation procedure of reference 1 the expression

$$C = \frac{F_C}{F_I} (F_I + iG_I)$$

was used for the complex circulation function. In this expression

UNCLASSIFIED

CONFIDENTIAL

11

$$F_C = \frac{(2l'_\alpha - l'_z) + \frac{k_{nr}}{2}(2l''_\alpha - l''_z) - \pi \frac{k_{nr}^2}{2}}{C_{l_{\alpha,n}} \left[1 + \left(\frac{k_{nr}}{2} \right)^2 \right]} \quad (6)$$

where l'_α , l'_z , l''_α , l''_z are aerodynamic coefficients given in reference 13 for two-dimensional airfoils oscillating in compressible flow, and $C_{l_{\alpha,n}}$ is the two-dimensional steady-flow lift-curve slope associated with the Mach number component M_{LE} normal to the leading-edge.

In the calculations of reference 1 linearized-theory values were used for the $C_{l_{\alpha,n}}$ in equation (6). That is,

$$\left. \begin{aligned} C_{l_{\alpha,n}} &= \frac{2\pi}{\beta_{LE}} \quad \text{for } M_{LE} < 1 \\ &= \frac{4}{\beta_{LE}} \quad \text{for } M_{LE} > 1 \end{aligned} \right\} \quad (7)$$

where $\beta_{LE} = \sqrt{M_{LE}^2 - 1}$. If equation (7) is used in equation (6), it can be seen that $F_C = 0$ for $M_{LE} = 1$. Consequently, a range of Mach number in the vicinity of $M_{LE} = 1$ is inaccessible to the method as presented in reference 1. The possibility of removing this limitation by using experimental values of two-dimensional steady-flow $C_{l_{\alpha,n}}$ in equation (6) is investigated herein for the two unswept wings with taper ratio of 0.6.

Experimental values of two-dimensional C_{l_α} for the NACA 65A004 airfoil were obtained from reference 14 over the Mach number range from 0.8 to 1.25. These values are reproduced here in figure 9. Figure 9 also shows the variation with Mach number of two-dimensional $\frac{C_{l_{\alpha,exp}}}{C_{l_{\alpha,theor}}}$. Values of F_C calculated by use of the theoretical values of equation (7) can be converted to the experimental C_{l_α} base (for the NACA 65A004 airfoil) by dividing the F_C by these values of $\frac{C_{l_{\alpha,exp}}}{C_{l_{\alpha,theor}}}$.

CONFIDENTIAL

RESULTS AND DISCUSSION

Presentation of Results

The wing configurations for which flutter calculations were made are summarized in table I. Table I also indicates the sources of the experimental steady-flow aerodynamic parameters used. Flutter characteristics have been calculated by use of experimentally determined spanwise distributions of steady-flow lift-curve slope and aerodynamic center (figs. 1 to 6) for five wings of aspect ratio 4.0, taper ratio 0.6, and quarter-chord sweep angles 0° and 45° . Flutter characteristics based on experimental total aerodynamic parameters (figs. 7 and 8) have been calculated for three unswept wings of aspect ratio 4.0 and taper ratio 0.6 and 1.0. Exploratory flutter calculations employing experimental two-dimensional steady-flow lift-curve slopes in the circulation functions for M_{LE} near 1 have been made for the two unswept wings of taper ratio 0.6. Structural data as well as experimental flutter data for all of these wings were obtained from references 1, 5, 6, and 12.

Since calculated flutter characteristics appear not to be very sensitive to slight changes in mode shapes, and since the wings of this study are not highly tapered, all flutter calculations presented herein were made by using the uncoupled mode shapes of a uniform cantilever beam. In all cases the first torsion mode and the first and second bending modes were used.

Unless otherwise indicated the subsequent discussion deals entirely with results obtained with circulation functions calculated by using theoretical two-dimensional lift-curve slopes (eq. (7)) as in references 1 and 15.

Wing designation.— The three-digit system used to identify the wings with taper ratio of 0.6 is the same as that used in references 1, 5, and 15. The first digit in this system is the aspect ratio of the full wing to the nearest integer. The second and third digits give the quarter-chord sweep angle to the nearest degree. For example, wing 445 has an aspect ratio of 4, a sweep angle of 45° , and a full-wing taper ratio of 0.6. Since some of the wings discussed in this paper have identical plan forms but different center-of-gravity positions (ref. 6), a single letter is appended to the plan-form designation to signify a forward or rearward shift in center of gravity. For example, wing 445 has a center of gravity at approximately 46 percent chord, whereas the center of gravity of wing 445F is at about 34 percent chord, and that of wing 445R is at about 58 percent chord. Wing 400 has a center of gravity at approximately 45 percent chord, but wing 400R has a center of gravity at about 59 percent chord.

For the wing with taper ratio of 1.0, the same system is used, except that a fourth digit 1 is added to distinguish the taper ratio. Thus wing 4001 has a full-wing aspect ratio of 4, a sweep angle of 0, and a taper ratio of 1.0.

Flutter characteristics.— Calculated flutter characteristics V/V_R and ω/ω_α are compared in figures 10 to 21 with experimental flutter data and with flutter characteristics calculated for the same wings in references 1 and 15 from theoretical distributions of aerodynamic parameters. The experimental flutter points shown were obtained at various values of density ρ , whereas, for a particular wing, all of the points calculated in this investigation and in reference 1 were obtained at a constant value of ρ which represented approximately an average of the experimental densities. For each experimental point, however, the normalizing V_R was calculated by using the appropriate experimental density. On the basis of previous experience, it appears that normalizing the experimental flutter speeds in this manner accounts for the major effects of density so that the resulting $(V/V_R)_{\text{exp}}$ is considered to depend only slightly on ρ , at least over the range of density variation which occurs herein. The variation of V/V_R with density is examined in detail in reference 15.

The reference flutter speeds V_R used in references 5 and 12 for wings 400 and 4001 were calculated by employing only two degrees of freedom (first bending and first torsion). Since three-degree-of-freedom calculations yield values of V_R which are slightly different from the two-degree-of-freedom values, the experimental V/V_R values for these two wings have been multiplied by the ratio
$$\frac{V_R \text{ (for two degrees of freedom)}}{V_R \text{ (for three degrees of freedom)}}$$
 so that both calculated and experimental flutter-speed ratios as presented herein are normalized by V_R for three degrees of freedom.

Swept Wings — Wings 445, 445F, 445R

Flutter speeds.— For wings 445, 445F, and 445R values of V/V_R (figs. 10 to 12) calculated from experimental distributions of $C_{l_{\alpha,n}}$ and ac_n (for the undeformed wing in steady flow) (figs. 1 and 2) are in good agreement with experimental V/V_R values at subsonic, transonic, and supersonic speeds and are also in good agreement at subsonic and supersonic speeds with values calculated from theoretical distributions

of $C_{l_{\alpha,n}}$ and ac_n (refs. 1 and 15)¹. When comparing flutter characteristics obtained from these three sources, however, it should be remembered that the experimental distributions of $C_{l_{\alpha,n}}$ and ac_n used were obtained from data for a 6-percent-thick wing while the experimental flutter points were obtained with 4-percent-thick wings. It is observed that the dip which appears in the V/V_R curves (figs. 10 to 12) in the range $0.8 < M < 1.0$ is coincident with a relatively sharp forward shift in ac_n position for the 6-percent-thick wing (fig. 3). Since this ac_n shift might be expected to be somewhat less severe for a 4-percent-thick wing, use of experimental aerodynamic parameters for a 4-percent-thick wing might be expected to result in a somewhat shallower dip in the V/V_R curves. The above-mentioned effect of ac_n change is believed to be the principal inaccuracy resulting from use of aerodynamic parameters for a 6-percent-thick wing. Figure 3 shows that the values of $C_{l_{\alpha,n}}$ and ac_n for $M = 0.94$ and $M = 0.96$ differ significantly from the curves faired through the remainder of the data. Because of this deviation the flutter points calculated for these two Mach numbers have been ignored in fairing the V/V_R curves in figures 10 to 12.

Figure 10 shows flutter speeds for wing 445 at supersonic Mach numbers calculated from experimental distributions of $C_{l_{\alpha,n}}$ and ac_n obtained both by directly applying equations (1) and (2) to data for streamwise sections (solid curves of figs. 1 and 2) and by adapting these values near the tip to the strip orientation employed in the flutter calculation procedure as described previously (dashed curves of figs. 1 and 2). The flutter speeds resulting from these two methods of evaluating $C_{l_{\alpha,n}}$ and ac_n are so close together that use of the strip-orientation adaptation is considered unnecessary at least for the wings of this investigation. Accordingly, for wings 445F and 445R equations (1) and (2) are applied directly for all Mach numbers.

Figure 10 also shows flutter speeds at subsonic Mach numbers calculated by using circulation functions for incompressible flow ($C = F_I + iG_I$). It appears that subsonic flutter speeds calculated in this manner for wing 445 are low by no more than about 5 percent up to $M = 0.90$. This result further confirms the statement in reference 1 that the modified

¹For the subsonic points calculated from theoretical aerodynamic parameters the value of ac_n has been obtained from equation (2) with $ac = \frac{1}{4}$ as discussed in reference 15. The V/V_R and ω/ω_α curves shown in figures 10 to 21 are identical to those of reference 15.

circulation function $C = \frac{F_C}{F_I}(F_I + iG_I)$ need be employed only at high subsonic and supersonic speeds. Reference 15 discusses this point further in connection with flutter calculations employing theoretical distributions of $C_{l_{\alpha,n}}$ and ac_n .

Flutter frequencies.- For the three 45° swept wings values of ω/ω_α (figs. 13 to 15) calculated from experimental distributions of $C_{l_{\alpha,n}}$ and ac_n are in good agreement with experimental ω/ω_α values at subsonic and transonic speeds and are also in good agreement at subsonic and supersonic speeds with values calculated from theoretical distributions of $C_{l_{\alpha,n}}$ and ac_n (refs. 1 and 15). For all three wings at transonic speeds the ω/ω_α curves calculated from experimental aerodynamic parameters turn upward tending to follow the trend of the experimental ω/ω_α values. At Mach numbers past 1.0, however, the upward trend is halted, and the curves then tend to follow those calculated from theoretical aerodynamic parameters.

Figure 13 shows flutter frequencies for wing 445 at supersonic Mach numbers calculated from experimental distributions of $C_{l_{\alpha,n}}$ and ac_n obtained both by directly applying equations (1) and (2) to data for streamwise sections (solid curves of figs. 1 and 2) and by adapting these values near the tip to the strip orientation employed in the flutter calculation procedure (dashed curves of figs. 1 and 2). The closeness of the frequencies which result from these two methods of evaluating $C_{l_{\alpha,n}}$ and ac_n confirms the statement (made previously in connection with flutter speeds) that the strip-orientation adaptation is unnecessary here.

Figure 13 also shows flutter frequencies at subsonic Mach numbers calculated by using circulation functions for incompressible flow ($C = F_I + iG_I$). The differences between these frequencies and those calculated by using the modified circulation function $C = \frac{F_C}{F_I}(F_I + iG_I)$ are very small for all subsonic Mach numbers.

Unswept Wings with Taper Ratio of 0.6 — Wings 400, 400R

Flutter speeds.- For wings 400 and 400R values of V/V_R (figs. 16 and 17) at $M = \sqrt{2}$, calculated from distributions of $C_{l_{\alpha,n}}$ and ac_n

obtained from flight tests of the X-1E airplane, are in much better agreement with the experimental flutter data than are the values calculated from linearized-theory aerodynamic parameters, especially for wing 400. The distributions of $C_{l_{\alpha,n}}$ and ac_n obtained from the X-1E data are compared with values calculated from steady-flow linearized theory in figure 6. This comparison shows that the $C_{l_{\alpha,n}}$ distribution is accurately predicted by linearized theory except near the fuselage. However, as might be expected the linearized theory predicts aerodynamic-center positions that are too far rearward. References 1 and 15 hypothesized that for wing 400 at supersonic Mach numbers the poor agreement between experimental flutter speeds and those calculated from steady-flow linearized-theory aerodynamics was related to the close proximity of the local aerodynamic centers to the local centers of gravity and to the fact that linear theory predicts too-far rearward aerodynamic centers. For wing 400 at supersonic Mach numbers the great sensitivity of calculated flutter speed to small changes in aerodynamic-center position was demonstrated in reference 15. Comparison of the flutter speeds calculated from the X-1E data and from linearized-theory aerodynamic parameters gives further evidence of this sensitivity. In view of this sensitivity and in view of the fact that the differences in aerodynamic center shown in figure 6 are caused by finite wing thickness, viscosity, and other nonlinear effects, it seems doubtful that accurate supersonic flutter speeds for this wing could be obtained by using any linearized theory.

For wings 400 and 400R, values of V/V_R (figs. 16 and 17) calculated from $C_{l_{\alpha,n}}$ and ac_n distributions obtained from the data of reference 7 (fig. 4) appear to be consistent with the experimental flutter points for Mach numbers up to 0.8. Since $M_{LE} \approx M$ for these unswept wings, and since the circulation function F_C approaches 0 as M_{LE} approaches 1, the Mach number range near $M \approx M_{LE} = 1.0$ for these wings is not accessible to the calculation procedure as given in reference 1. (See previous discussion of this point.) As shown in figures 16 and 17 for Mach numbers near 1.0, the calculated flutter speeds appear to increase without limit.

As indicated previously, an attempt was made to eliminate this spurious behavior of the V/V_R curves by employing experimental values of the two-dimensional lift-curve slope (fig. 9) in the calculation of the circulation function F_C for Mach numbers near 1.0 (M_{LE} near 1.0). The V/V_R values obtained in this manner are shown in figures 16 and 17. It may be seen that although finite V/V_R values are obtained for $M = 1.0$, the agreement with experimental V/V_R values still is not good.

Accordingly, the artifice employed in the computation of the circulation functions for these flutter calculations is not used further.

Values of V/V_R for wings 400 and 400R calculated by using total lift-curve slope and aerodynamic center (fig. 7) as described previously are shown in figures 16 and 17. These values are in good agreement with the experimental values up to $M = 0.8$. Above this Mach number the limitation on the circulation function just discussed is again indicated by a spurious rise in the calculated flutter speed.

Flutter frequencies.— For wings 400 and 400R values of ω/ω_α (figs. 18 and 19) at $M = \sqrt{2}$, calculated from distributions of $C_{l_{\alpha,n}}$ and ac_n obtained from flight tests of the X-1E airplane (fig. 6), are in good agreement with the experimental flutter frequencies. Comparing these calculated frequencies with those calculated from linearized-theory aerodynamic parameters (refs. 1 and 15) shows that use of aerodynamic parameters for the X-1E airplane results in a very large frequency reduction for wing 400 but only an insignificant reduction for wing 400R. This large frequency change for wing 400 again indicates the great sensitivity of calculated supersonic flutter characteristics for that wing to small changes in aerodynamic-center position. (See previous discussion of flutter speeds and reference 15.) Flutter frequencies for wings 400 and 400R calculated by use of steady-flow aerodynamic parameters obtained from the data of reference 7 (fig. 4) are somewhat closer to the experimental flutter frequencies than are the curves faired through points calculated from linear-theory aerodynamic parameters. Flutter frequencies for these two wings calculated by use of experimental values of total aerodynamic parameters (fig. 7) closely follow the values calculated from distributions of linear-theory aerodynamic parameters.

Unswept Wing with Taper Ratio of 1.0 — Wing 4001

Flutter speeds.— Values of V/V_R for wing 4001 calculated by using total lift-curve slope and aerodynamic center (fig. 8) are shown in figure 20. These values are in fairly good agreement with the experimental flutter points up to about $M = 0.85$, but above this Mach number a spurious asymptotic rise in the calculated flutter speed again appears as $M \rightarrow M_{LE}$ approaches 1.0. It should be remembered that the aerodynamic parameters of figure 8 were obtained with wings with NACA 63A004 and NACA 65A004 airfoil sections (rounded leading edge), while the experimental flutter points were obtained with wings with a 4-percent-thick hexagonal airfoil (sharp leading edge). It is recognized that even though the wings of figure 8 and reference 12 have the same thickness, these differences of airfoil shape (especially leading-edge radius) can

lead to significant differences in the lift-curve slope and aerodynamic center, particularly at Mach numbers near 1.0. At high subsonic speeds, for example, it is probable that the aerodynamic center for the flutter wings was slightly farther rearward than the positions indicated in figure 8. If properly accounted for this condition would result in calculated flutter speeds slightly higher than those shown in figure 20.

Flutter frequencies.- Flutter frequencies (fig. 21) calculated by using the aerodynamic parameters of figure 8 are slightly lower than frequencies calculated by using linear-theory aerodynamic parameters, particularly at high subsonic and transonic speeds.

CONCLUDING REMARKS

Flutter calculations for several swept and unswept wings through the transonic speed range have been made by the modified strip-theory method of NACA RM L57L10, which employs steady-flow aerodynamic parameters for the undeformed wing. Experimentally determined distributions of steady-flow aerodynamic parameters for the undeformed wings were used in the present calculations. Comparisons of these calculated results with experimental flutter data and with calculations previously made by using linearized-theory static aerodynamic parameters indicate that the method employed gives accurate flutter results for swept wings at subsonic, transonic, and supersonic speeds. However, since this method of flutter calculation is not applicable when the Mach number component normal to the leading edge is near 1.0, it appears that the transonic flutter characteristics of unswept wings cannot be calculated by the method as given in NACA RM L57L10. An attempt was made to remove this limitation by using experimental values of two-dimensional lift-curve slope (instead of theoretical values) in the calculation of circulation functions when the Mach number component normal to the leading edge was near 1.0. Applying this procedure to two unswept wings removed the spurious asymptotic rise of flutter speed near Mach number 1.0, but it did not result in very close agreement between calculated and experimental flutter speeds.

The possibility of obtaining estimates of flutter characteristics for unswept wings by use of total aerodynamic parameters has also been examined. Although no supersonic calculations were made using total aerodynamic parameters, it appears that the procedure outlined gives reasonable estimates of flutter characteristics at subsonic speeds.

Langley Research Center,
National Aeronautics and Space Administration,
Langley Field, Va., August 26, 1959.

CONFIDENTIAL

REFERENCES

1. Yates, E. Carson, Jr.: Calculation of Flutter Characteristics for Finite-Span Swept or Unswept Wings at Subsonic and Supersonic Speeds by a Modified Strip Analysis. NACA RM L57L10, 1958.
2. Runyan, Harry L., and Woolston, Donald S.: Method for Calculating the Aerodynamic Loading on an Oscillating Finite Wing in Subsonic and Sonic Flow. NACA Rep. 1322, 1957. (Supersedes NACA TN 3694.)
3. Loving, Donald L., and Estabrooks, Bruce B.: Transonic-Wing Investigation in the Langley 8-Foot High-Speed Tunnel at High Subsonic Mach Numbers and at a Mach Number of 1.2. Analysis of Pressure Distribution of Wing-Fuselage Configuration Having a Wing of 45° Sweepback, Aspect Ratio 4, Taper Ratio 0.6, and NACA 65A006 Airfoil Section. NACA RM L51F07, 1951.
4. Loving, Donald L., and Williams, Claude V.: Aerodynamic Loading Characteristics of a Wing-Fuselage Combination Having a Wing of 45° Sweepback Measured in the Langley 8-Foot Transonic Tunnel. NACA RM L52B27, 1952.
5. Unangst, John R., and Jones, George W., Jr.: Some Effects of Sweep and Aspect Ratio on the Transonic Flutter Characteristics of a Series of Thin Cantilever Wings Having a Taper Ratio of 0.6. NACA RM L55I13a, 1956.
6. Jones, George W., Jr., and Unangst, John R.: Investigation To Determine Effects of Center-of-Gravity Location on Transonic Flutter Characteristics of a 45° Sweptback Wing. NACA RM L55K30, 1956.
7. Hieser, Gerald, Henderson, James H., and Swihart, John M.: Transonic Aerodynamic and Loads Characteristics of a 4-Percent-Thick Unswept-Wing-Fuselage Combination. NACA RM L54B24, 1954.
8. DeYoung, John, and Harper, Charles W.: Theoretical Symmetric Span Loading at Subsonic Speeds for Wings Having Arbitrary Plan Form. NACA Rep. 921, 1948.
9. Myers, Boyd C., II, and Wiggins, James W.: Aerodynamic Characteristics of a Wing With Unswept Quarter-Chord Line, Aspect Ratio 4, Taper Ratio 0.6, and NACA 65A004 Airfoil Section. Transonic-Bump Method. NACA RM L50C16, 1950.
10. Hammond, Alexander D.: Wind-Tunnel Investigation of the Effect of Aspect Ratio and Chordwise Location on Effectiveness of Plain Spoilers on Thin Untapered Wings at Transonic Speeds. NACA RM L56F20, 1956.

11. Nelson, Warren H., and McDevitt, John B.: The Transonic Characteristics of 22 Rectangular, Symmetrical Wing Models of Varying Aspect Ratio and Thickness. NACA TN 3501, 1955. (Supersedes NACA RM A51A12.)
12. Pratt, George L.: Experimental Flutter Investigation of a Thin Unswept Wing at Transonic Speeds. NACA RM L55A18, 1955.
13. Jordan, P. F.: Aerodynamic Flutter Coefficients for Subsonic, Sonic, and Supersonic Flow (Linear Two-Dimensional Theory). Rep. No. Structures 141, British R.A.E., Apr. 1953.
14. Ladson, Charles L.: Two-Dimensional Airfoil Characteristics of four NACA 6A-Series Airfoils at Transonic Mach Numbers up to 1.25. NACA RM L57F05, 1957.
15. Yates, E. Carson, Jr.: Some Effects of Variations in Density and Aerodynamic Parameters on the Calculated Flutter Characteristics of Finite-Span Swept and Unswept Wings at Subsonic and Supersonic Speeds. NASA TM X-182, 1959.

CONFIDENTIAL

21

TABLE I.- SUMMARY OF CONFIGURATIONS FOR WHICH FLUTTER CALCULATIONS WERE MADE INCLUDING SOURCES OF THE EXPERIMENTAL STATIC AERODYNAMIC PARAMETERS USED

Wing designation	Configuration for which flutter tests and flutter calculations were made				Source of experimental static aerodynamic parameters					Use of experimental aerodynamic parameters	Flutter results presented herein in figure		
	Aspect ratio	Sweep angle (quarter-chord), deg	Taper ratio	Airfoil section (stream-wise)	Center of gravity, percent chord	Reference in which presented	Figure herein	Aspect ratio	Sweep angle, deg			Taper ratio	Airfoil section (stream-wise)
4-5	4.0	45	0.6	NACA 65A004	46	3, 4	1, 2, 3	4.0	$\Lambda_c/4 = 45$	0.6	NACA 65A006	Spanwise distributions	10, 13
4-5F					34	3, 4	1, 2, 3	4.0	$\Lambda_c/4 = 45$.6	--do--	--do--	11, 14
4-5R					58	3, 4	1, 2, 3	4.0	$\Lambda_c/4 = 45$.6	--do--	--do--	12, 15
4-00	4.0	0	0.6	NACA 65A004	45	7	4, 5	4.0	$\Lambda_c/2 = 0$	0.6	NACA 65A004	Spanwise distributions	16, 18
4-00R					59	7	4, 5	4.0	$\Lambda_c/2 = 0$.6	--do--	--do--	17, 19
4-00					45	Unpublished	6	4.0	$\Lambda_{c,c} = 0$.6	NACA 65A004	--do--	16, 18
4-00R					59	Unpublished	6	4.0	$\Lambda_{c,c} = 0$.6	--do--	--do--	17, 19
4-00					45	9	7(a)	4.0	$\Lambda_c/4 = 0$.6	NACA 65A004	Total values	16, 18
4-00R					59	9	7(a)	4.0	$\Lambda_c/4 = 0$.6	--do--	--do--	17, 19
4-00					45	14	9	---	---	---	--do--	Two-dimensional C_{l_α} in F + iG	16, 18
4-00R					59	14	9	---	---	---	--do--	--do--	17, 19
4001	4.0	0	1.0	Hexagon	50	10	8(a)	4.0	$\Lambda = 0$	1.0	NACA 65A004	Total values	20, 21
					50	11	8(a)	4.0	$\Lambda = 0$	1.0	NACA 65A004	--do--	20, 21

CONFIDENTIAL

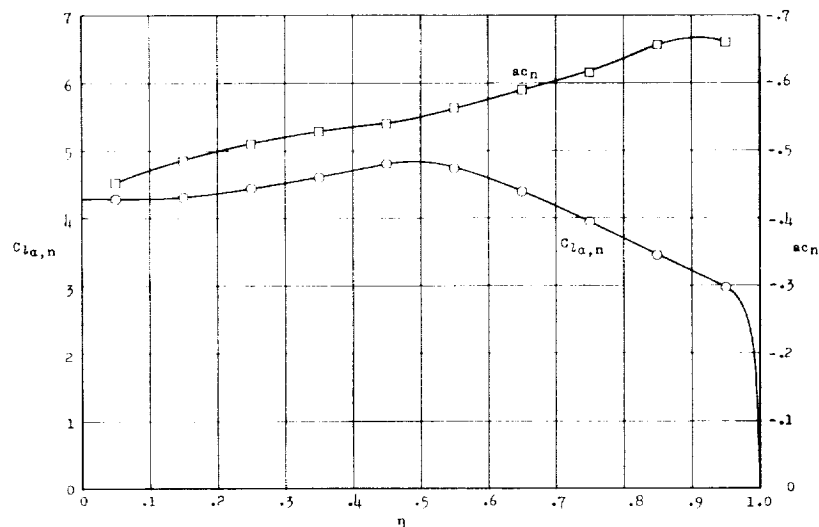
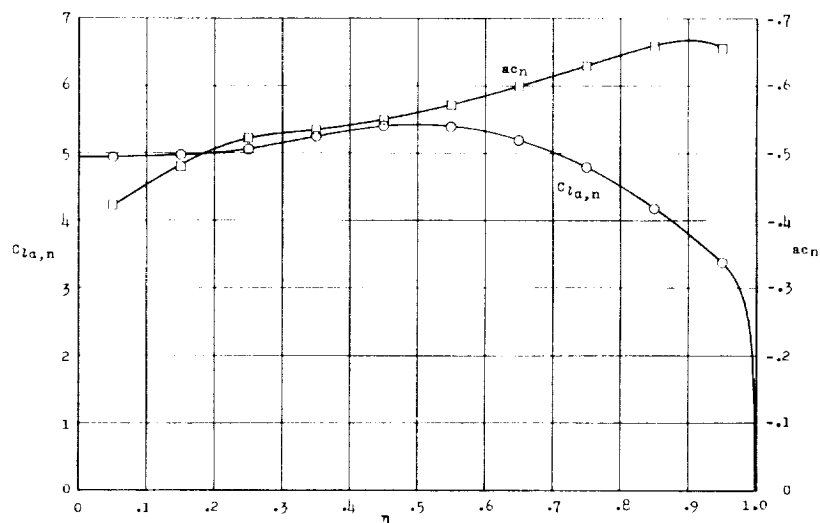
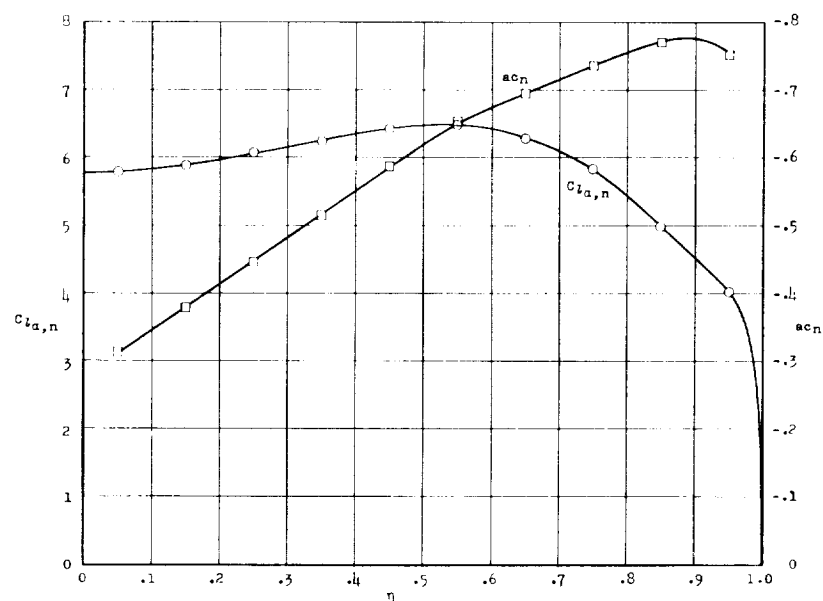
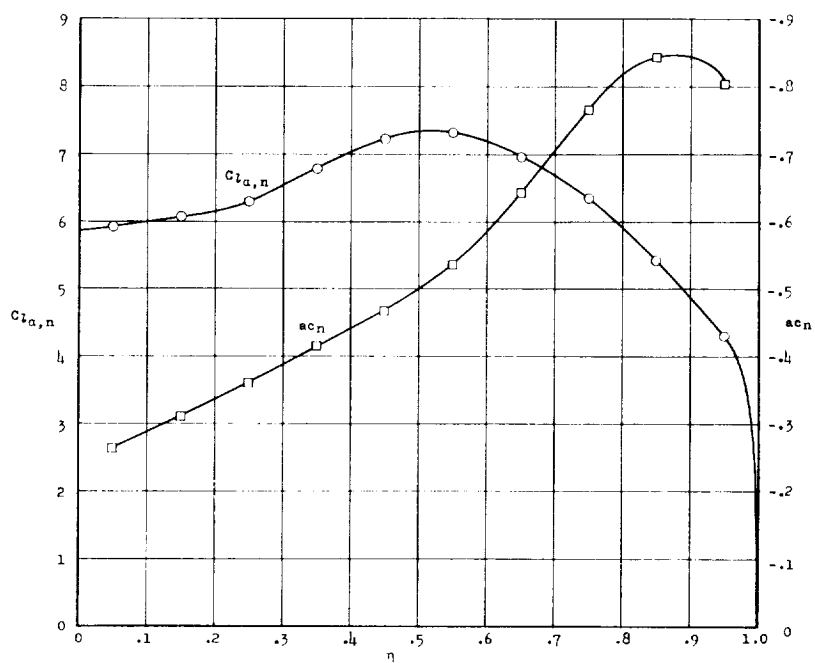
(a) $M = 0.60$.(b) $M = 0.80$.

Figure 1.- Distributions of steady-flow aerodynamic parameters obtained from the measured load distributions of reference 3 for a wing of $A = 4.0$, $\lambda = 0.6$, $\Lambda_c/4 = 45^\circ$, and NACA 65A006 airfoil. Symbols indicate values used in flutter calculations. Solid curves were obtained directly from equations (1) and (2). Dash curves were obtained by altering the results from equations (1) and (2) to conform to strip theory near the tip.

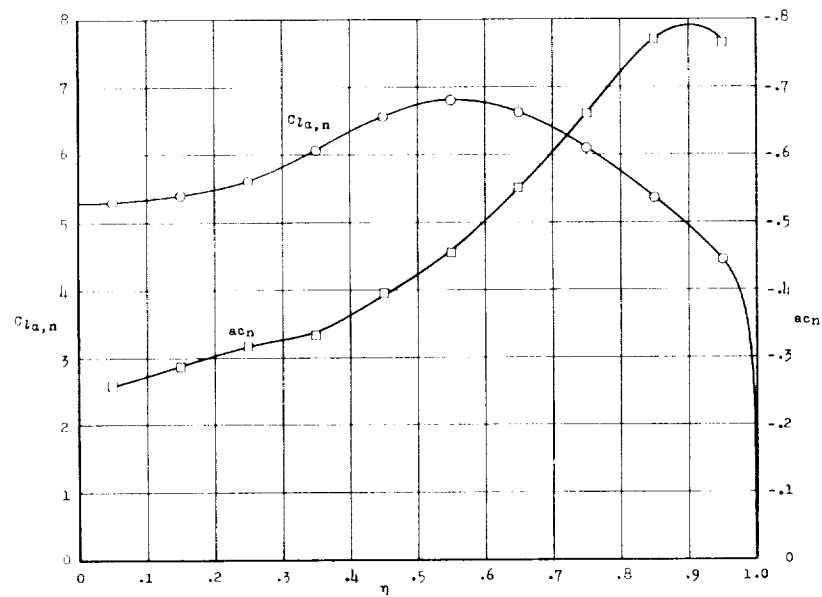


(c) $M = 0.90$.

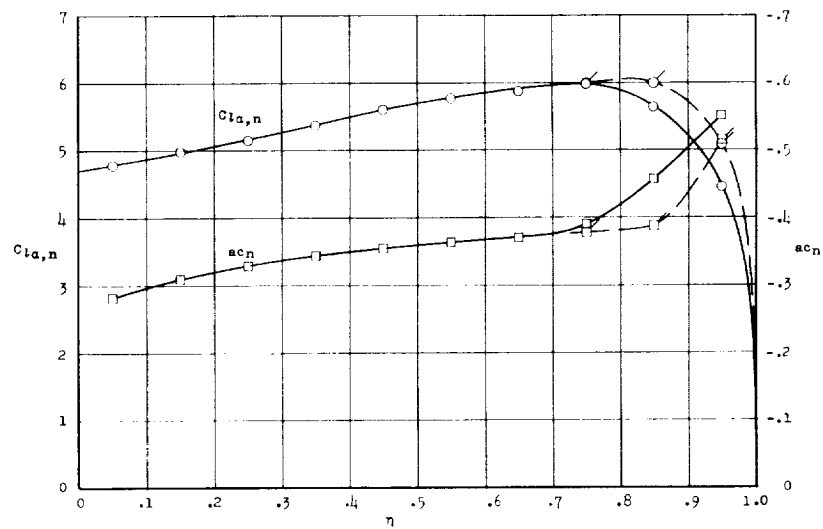


(d) $M = 0.93$.

Figure 1.- Continued.

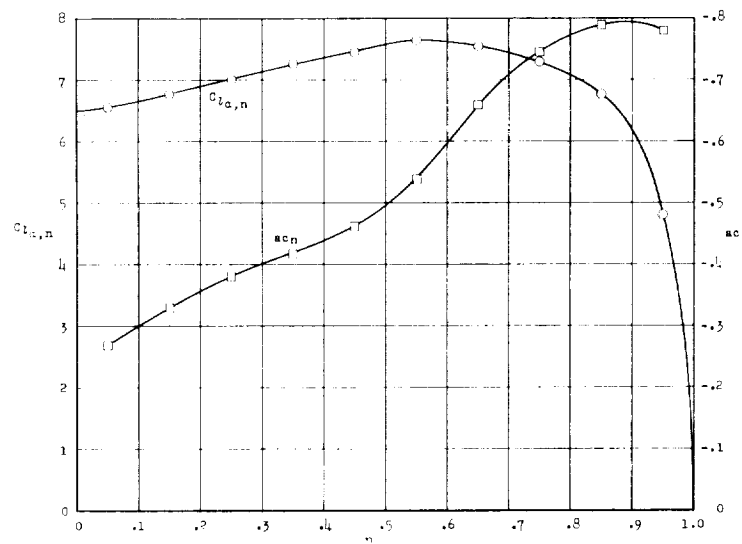


(e) $M = 0.96$.

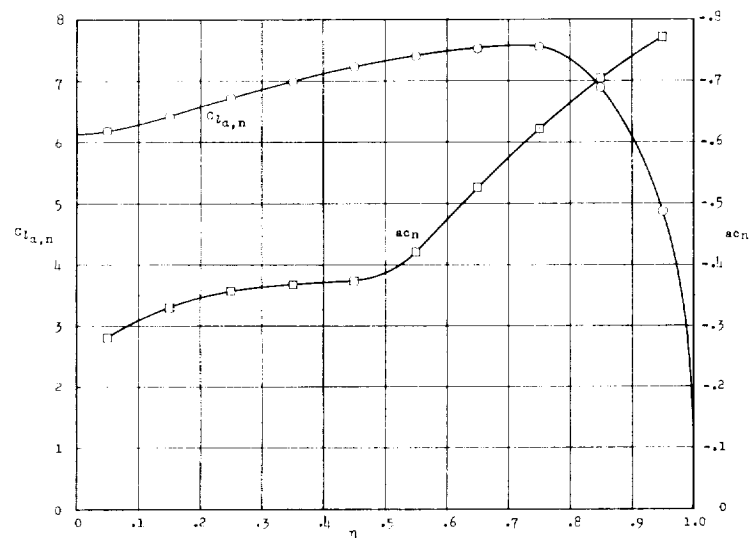


(f) $M = 1.20$.

Figure 1.- Concluded.



(a) $M = 0.94$.



(b) $M = 0.97$.

Figure 2.- Distributions of steady-flow aerodynamic parameters obtained from the measured load distributions of reference 4 for a wing of $A = 4.0$, $\lambda = 0.6$, $\Lambda_c/4 = 45^\circ$, and NACA 65A006 airfoil. Symbols indicate values used in flutter calculations. Solid curves were obtained directly from equations (1) and (2). Dash curves were obtained by altering the results from equations (1) and (2) to conform to strip theory near the tip.

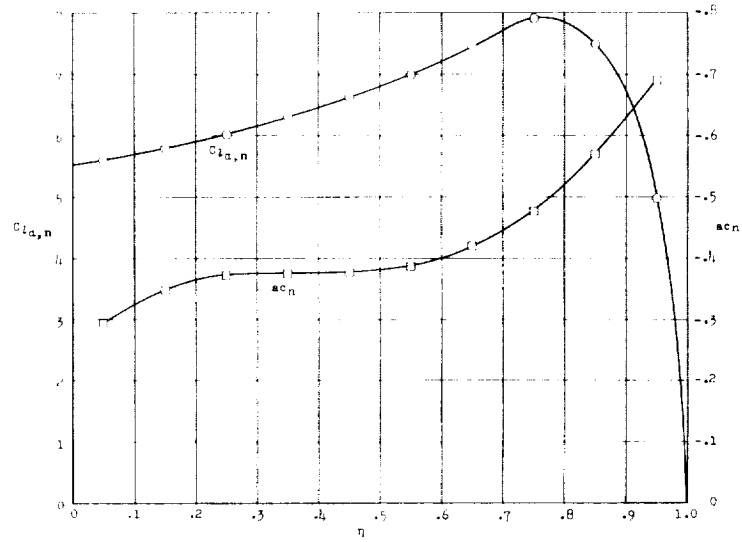
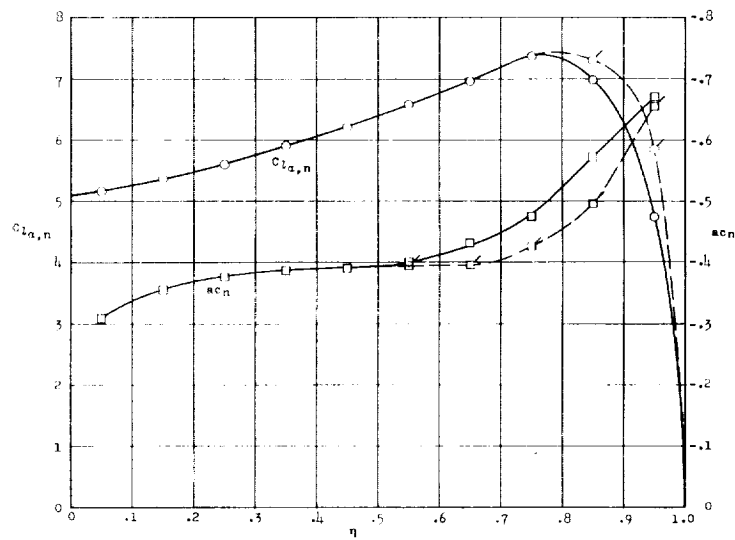
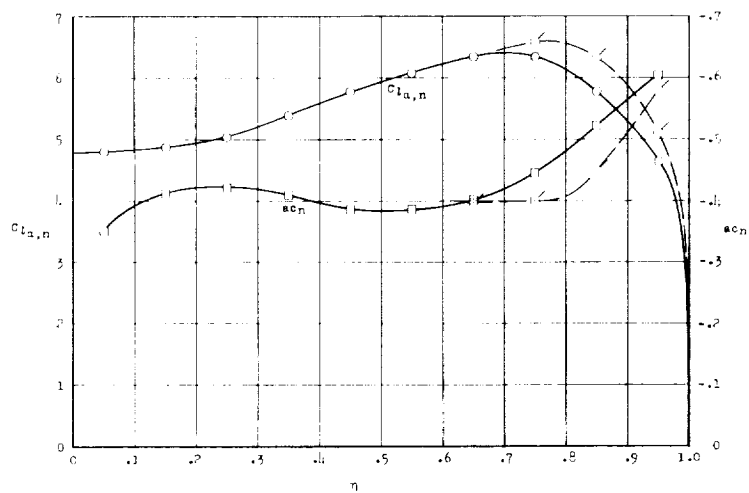
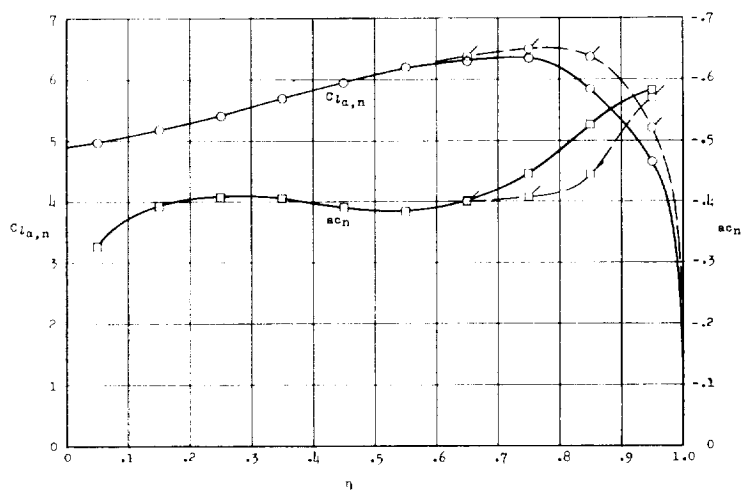
(c) $M = 0.99$.(d) $M = 1.02$.

Figure 2.- Continued.



(e) $M = 1.11$.



(f) $M = 1.13$.

Figure 2.- Concluded.

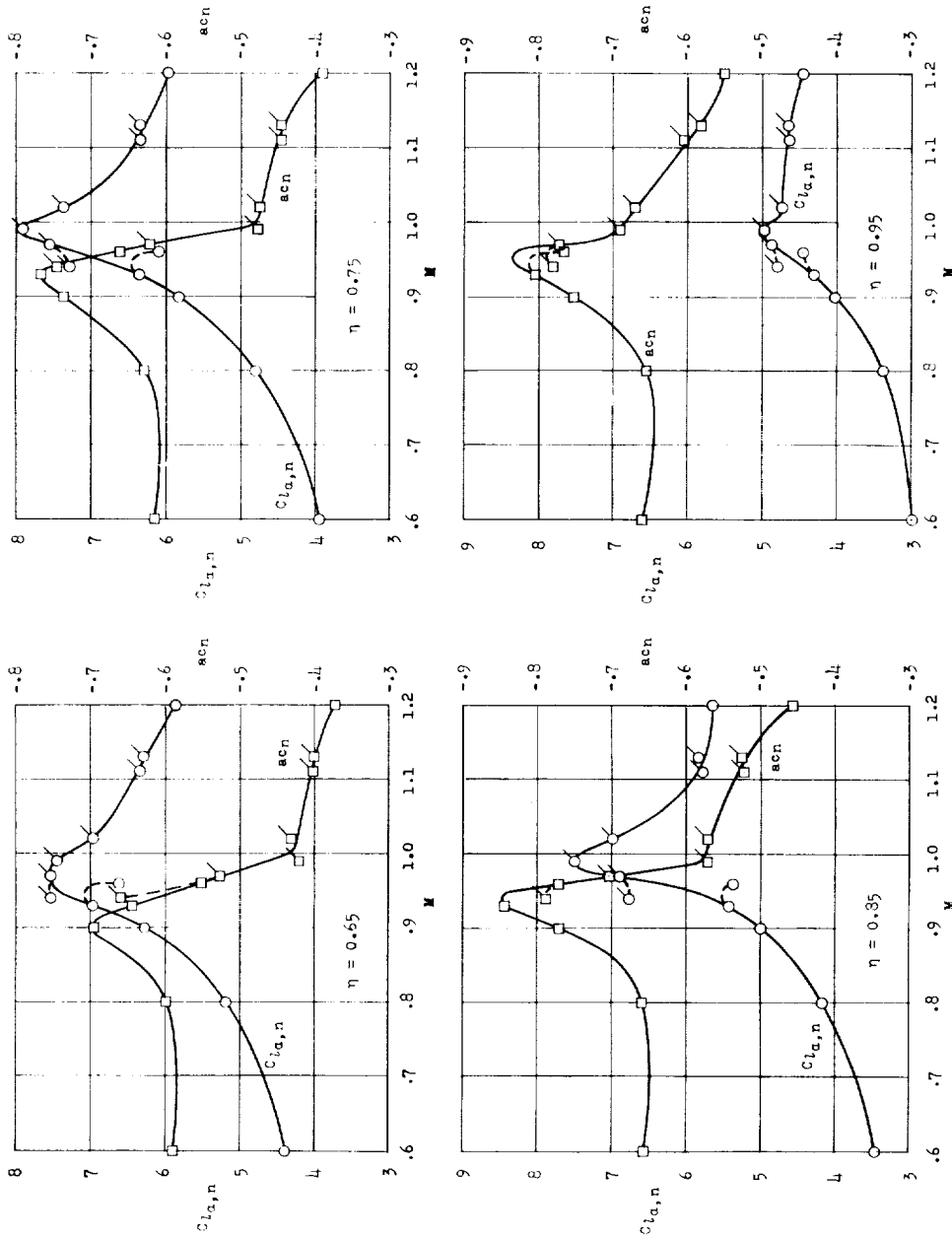
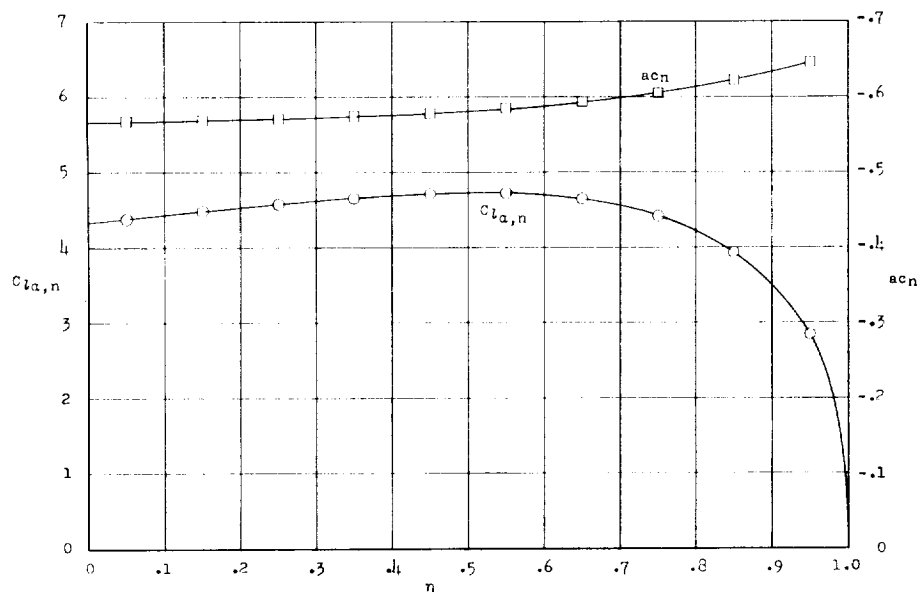
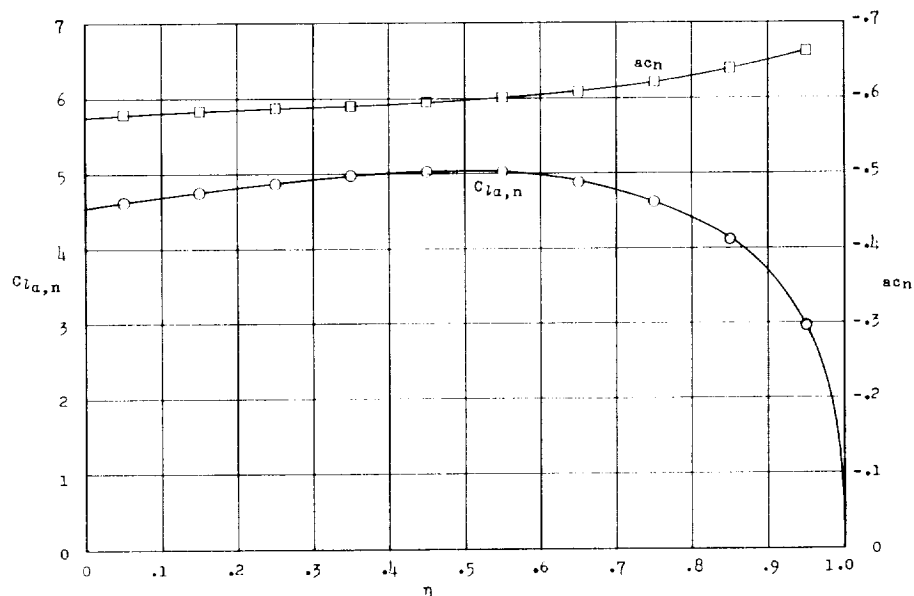


Figure 3.- Variation of steady-flow aerodynamic parameters with Mach number for several spanwise stations on the wing of reference 3 (plain symbols) and reference 4 (flagged symbols).
 $A = 4.0$; $\lambda = 0.6$; $\Lambda_c/4 = 45^\circ$; NACA 65A006 airfoil.



(a) $M = 0.60$.



(b) $M = 0.70$.

Figure 4.- Distribution of steady-flow aerodynamic parameters obtained from the measured pressure distributions of reference 7 for a wing of $A = 4.0$, $\lambda = 0.5$, $\Lambda_c/2 = 0$, and NACA 65A004 airfoil. Symbols indicate values used in flutter calculations.

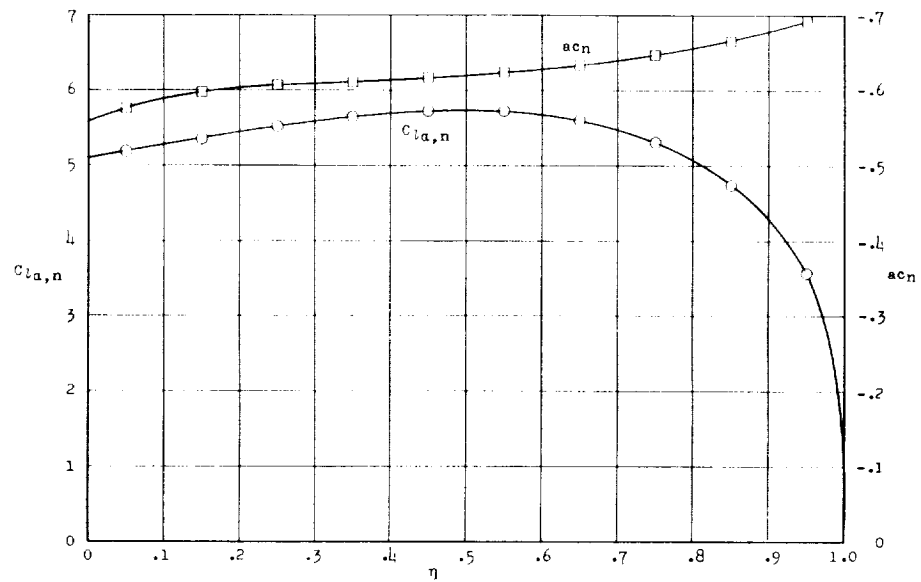
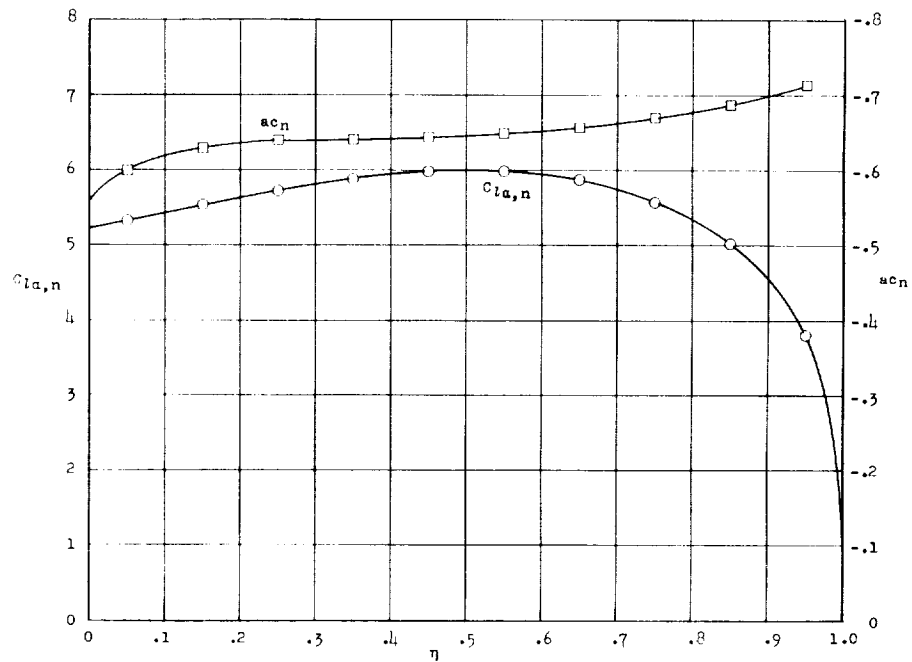
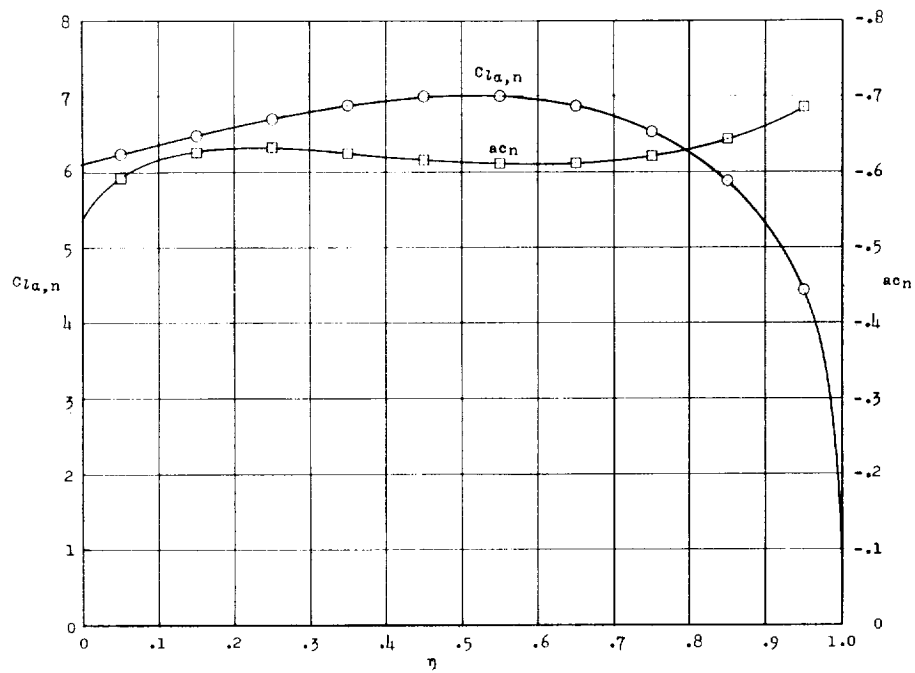
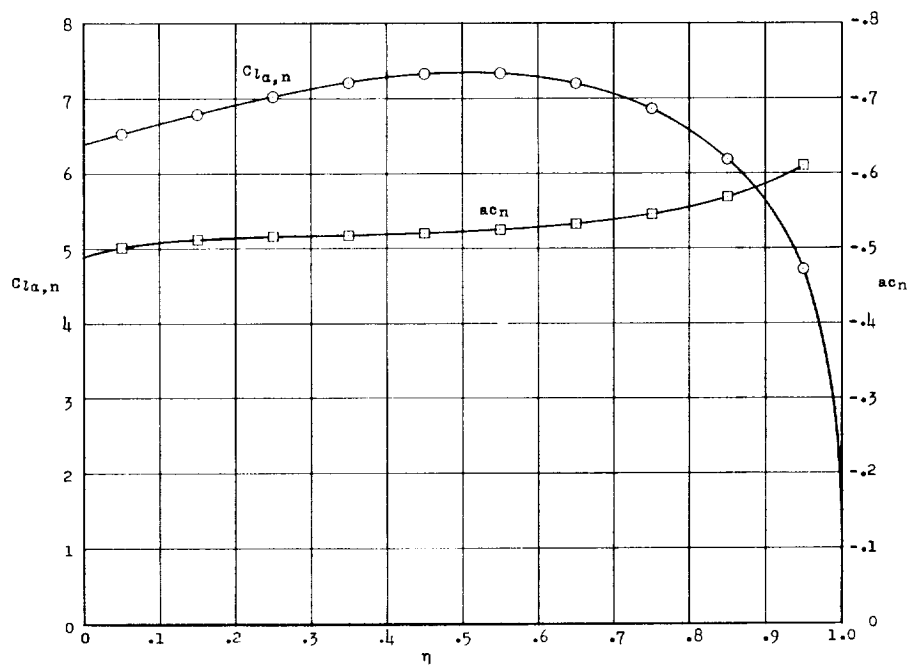
(c) $M = 0.80$.(d) $M = 0.85$.

Figure 4.- Continued.

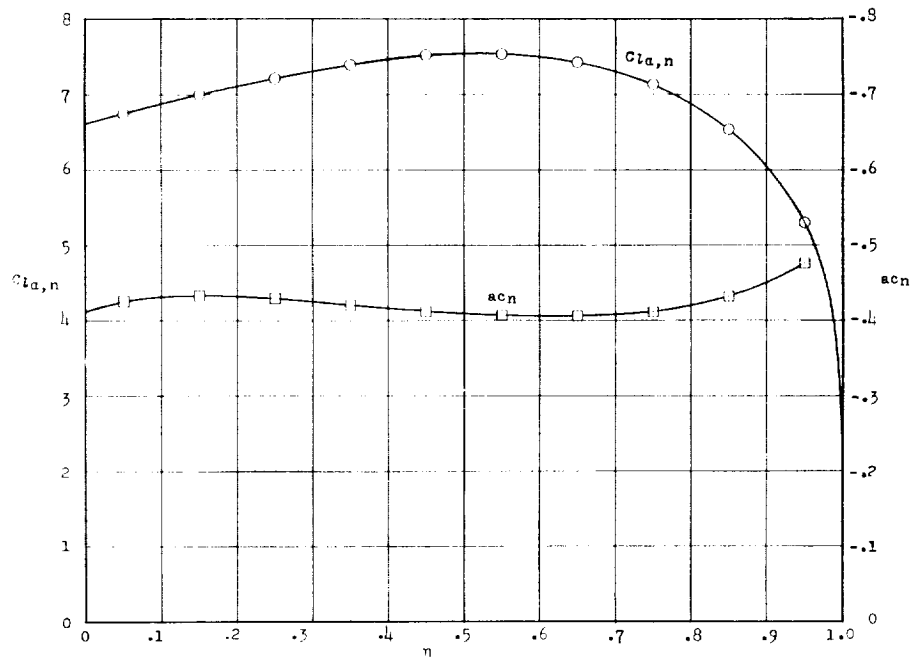


(e) $M = 0.88$.

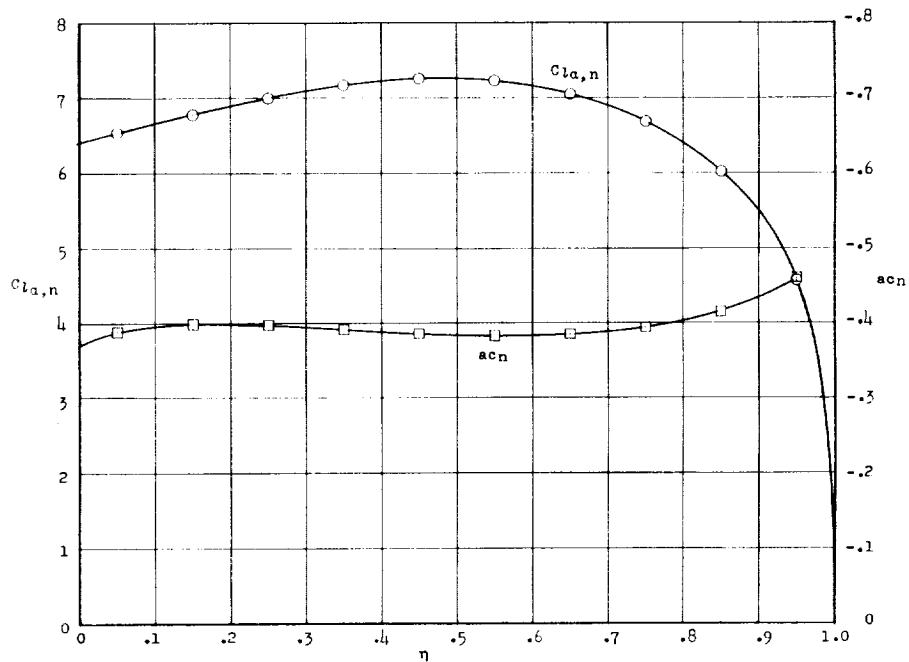


(f) $M = 0.90$.

Figure 4.- Continued.

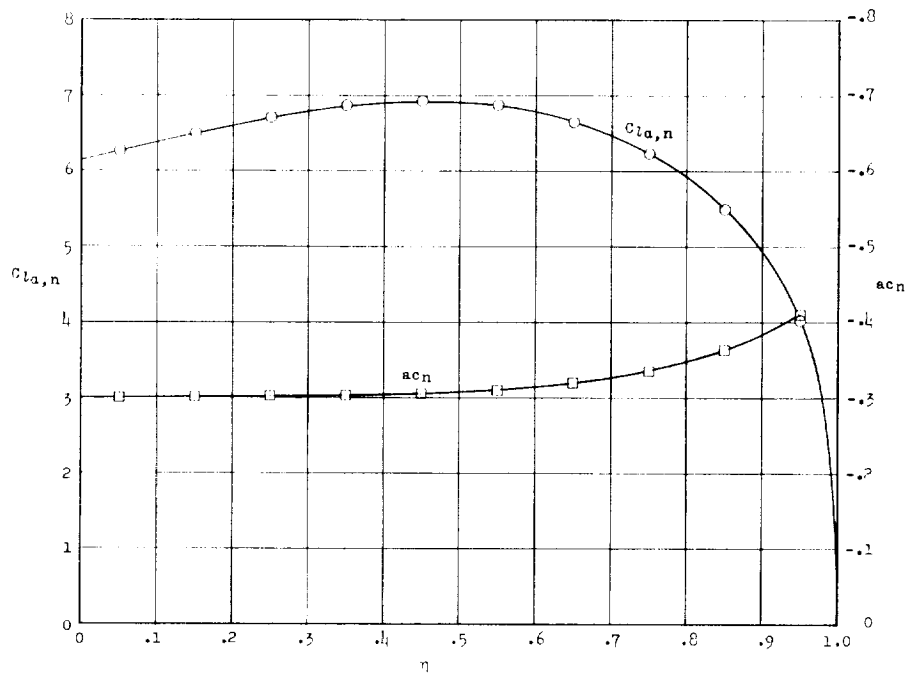


(g) $M = 0.92$.

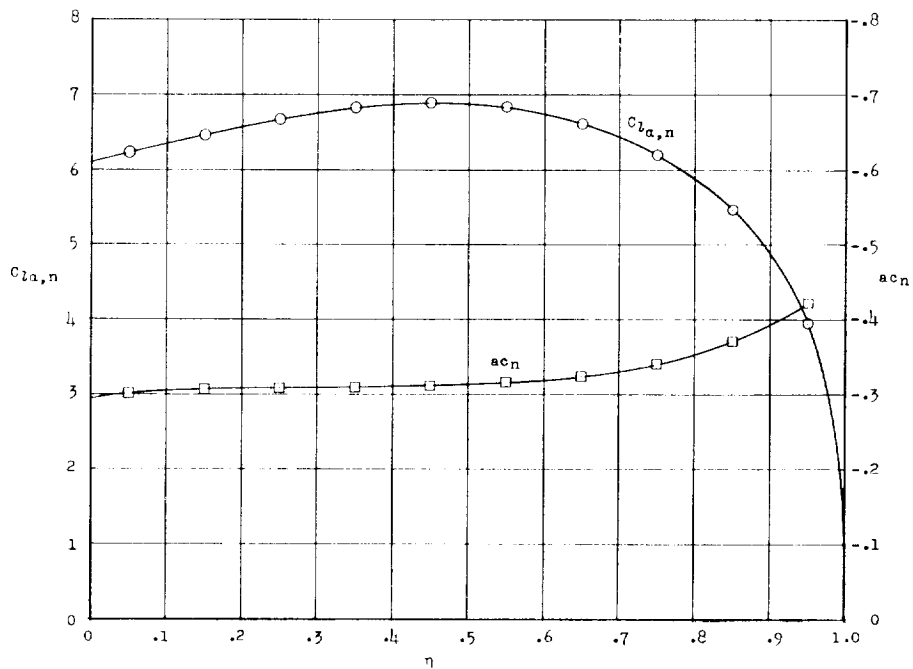


(h) $M = 0.94$.

Figure 4.- Continued.

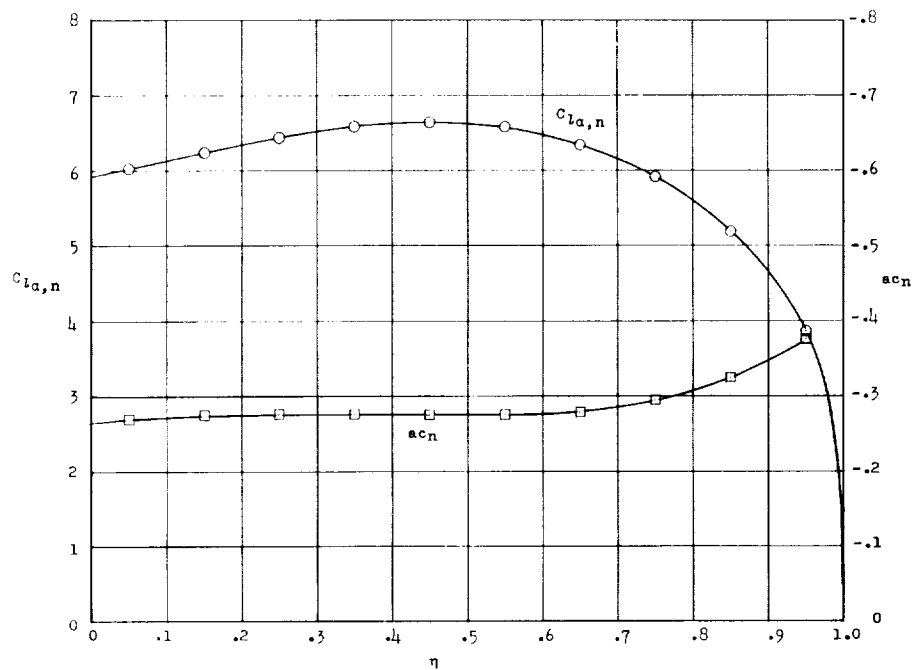


(i) $M = 0.96$.

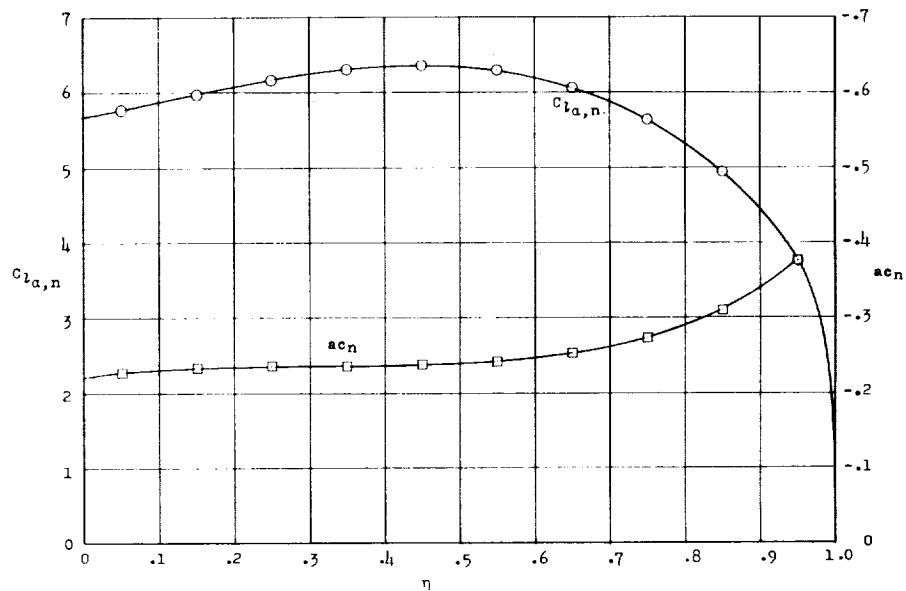


(j) $M = 0.98$.

Figure 4.- Continued.



(k) $M = 1.00$.



(l) $M = 1.05$.

Figure 4.- Concluded.

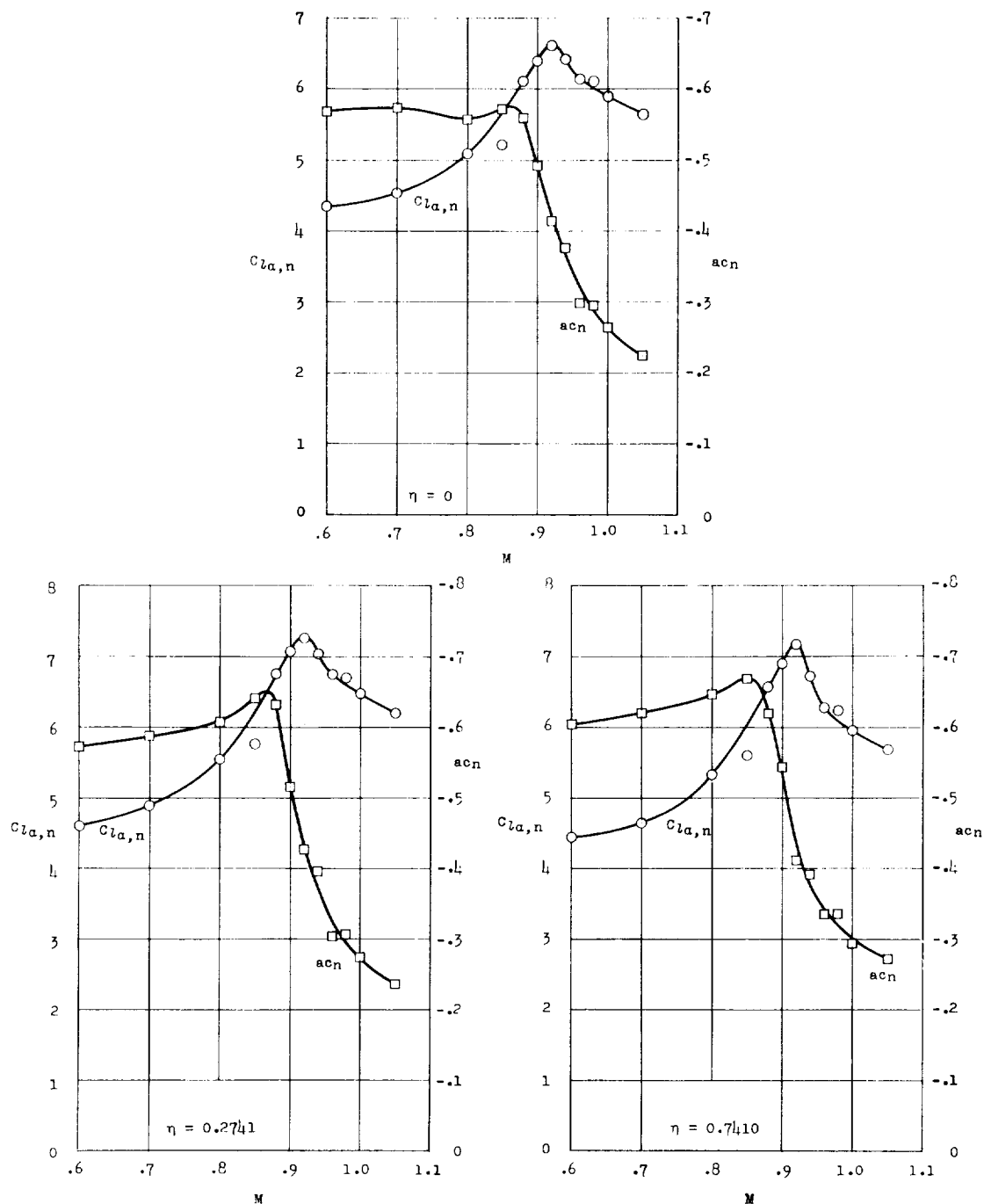


Figure 5.- Variation of steady-flow aerodynamic parameters with Mach number for three spanwise stations on the wing of reference 7.
 $A = 4.0$; $\lambda = 0.5$; $\Lambda_c/2 = 0$; NACA 65A004 airfoil.

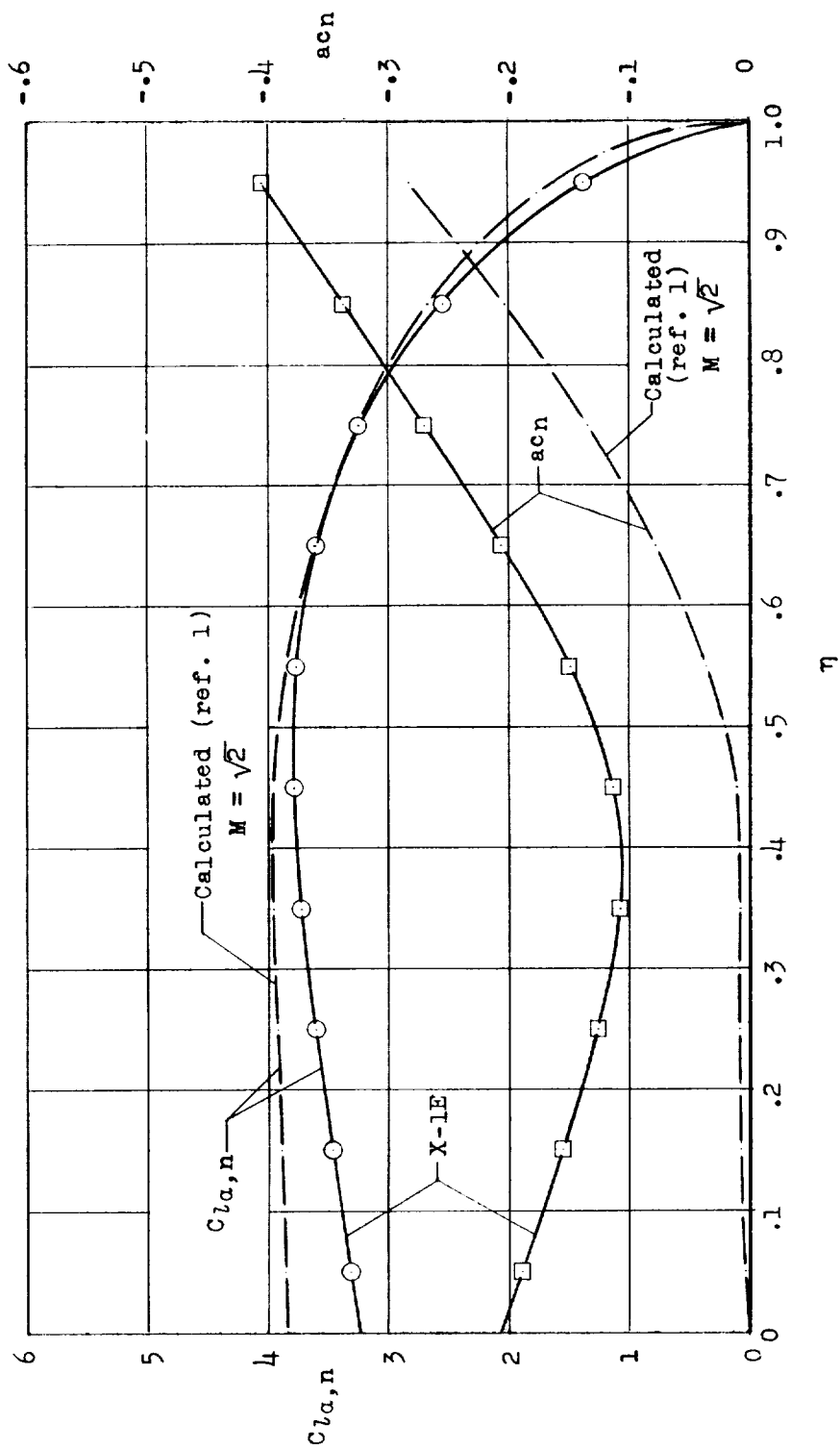
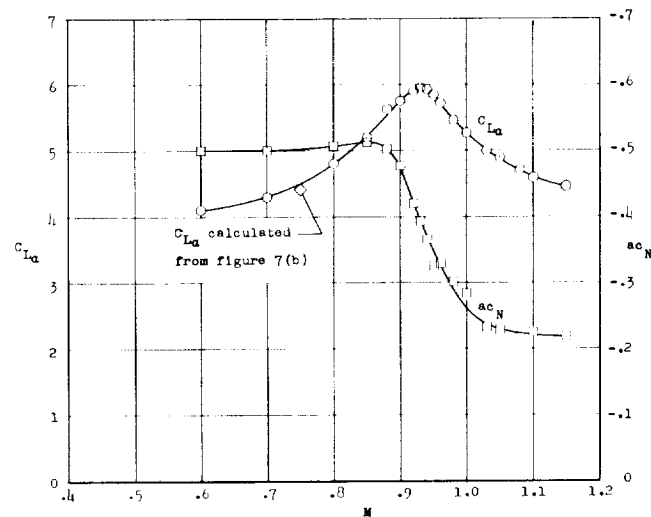
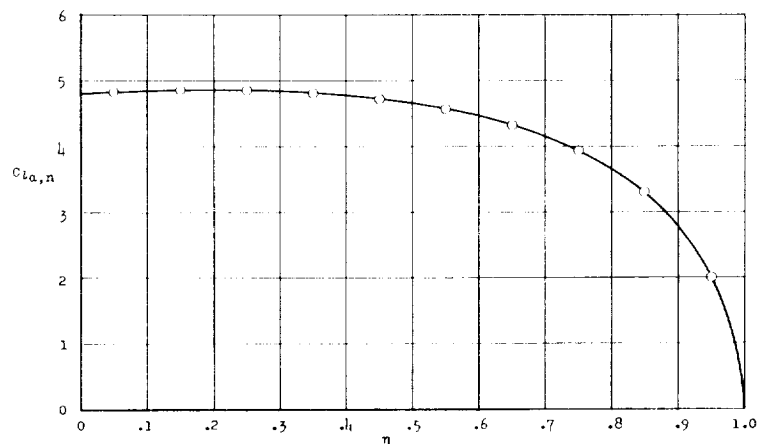


Figure 6.- Distributions of steady-flow aerodynamic parameters obtained from flight test data for the X-1E airplane at $M = 1.41$. $A = 4.0$; $\lambda = 0.5$; $\Delta_{1c} = 0$; modified NACA 64A004 airfoil. Symbols indicate values used in flutter calculations.

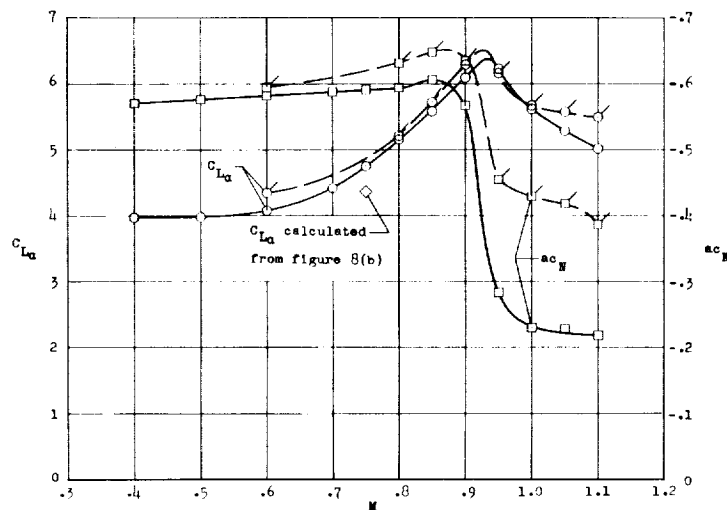


(a) Experimental steady-flow total aerodynamic parameters obtained from reference 9 for a wing of $A = 4.0$, $\lambda = 0.6$, $\Lambda_c/4 = 0$, and NACA 65A004 airfoil.

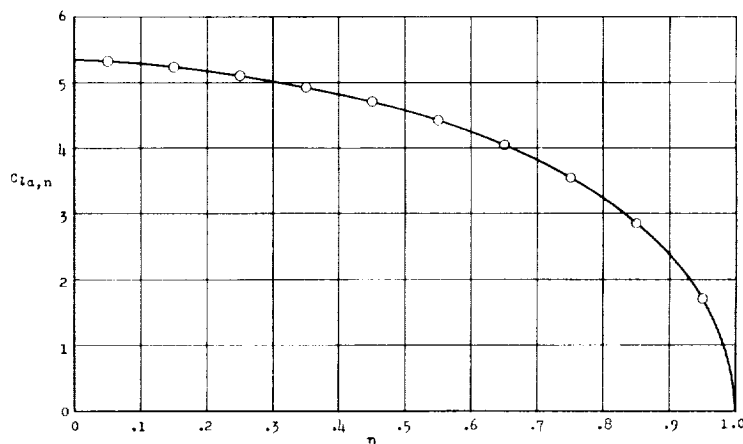


(b) Calculated spanwise distribution of $C_{La,n}$ which was used in combination with the experimental steady-flow total aerodynamic parameters of figure 7(a) in flutter calculations for wings 400 and 400R. Values of $C_{La,n}$ shown were calculated by the method of reference 8 for $M = 0.75$.

Figure 7.- Aerodynamic quantities involved in the estimation of flutter characteristics for wings 400 and 400R by use of total aerodynamic parameters.



(a) Experimental steady-flow total aerodynamic parameters for wings of $A = 4.0$, $\lambda = 1.0$, $\Lambda = 0$. Plain symbols represent data from reference 11 (wing with NACA 63A004 airfoil), and flagged symbols represent data from reference 10 (wing with NACA 65A004 airfoil).



(b) Calculated spanwise distribution of $C_{L\alpha,n}$ which was used in combination with the experimental steady-flow total aerodynamic parameters of figure 8(a) in flutter calculations for wing 4001. Values of $C_{L\alpha,n}$ shown were calculated by the method of reference 8 for $M = 0.75$.

Figure 8.- Aerodynamic quantities involved in the estimation of flutter characteristics for wing 4001 by use of total aerodynamic parameters.

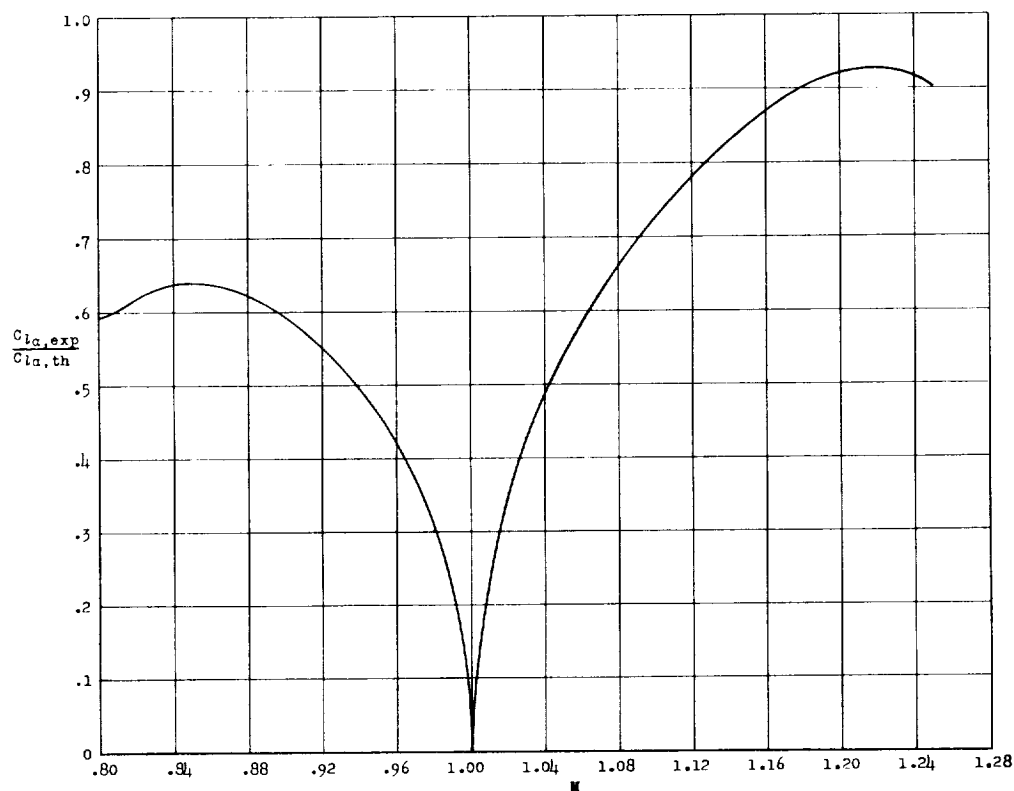
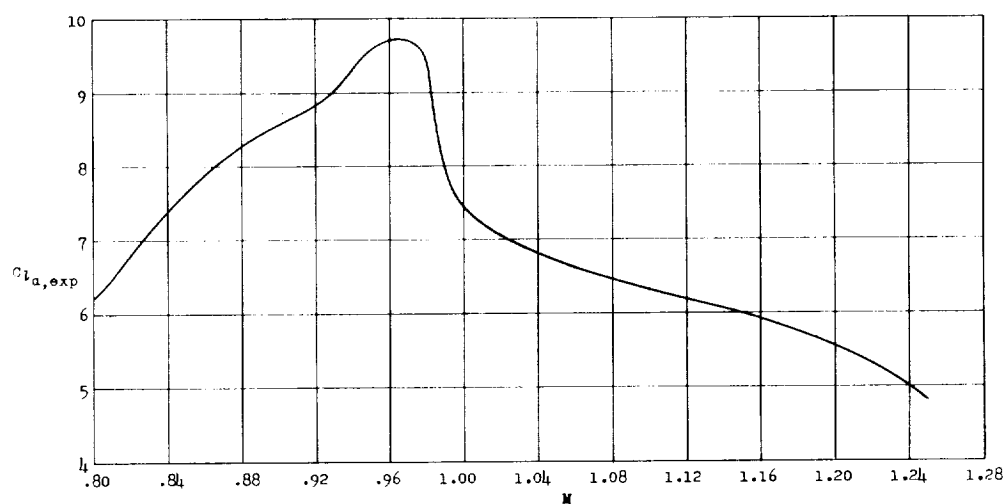


Figure 9.- Experimental two-dimensional steady-flow lift-curve slope for NACA 65A004 airfoil at zero lift as given in reference 14 and the relation of this quantity to linear-theory two-dimensional steady-flow lift-curve slope.

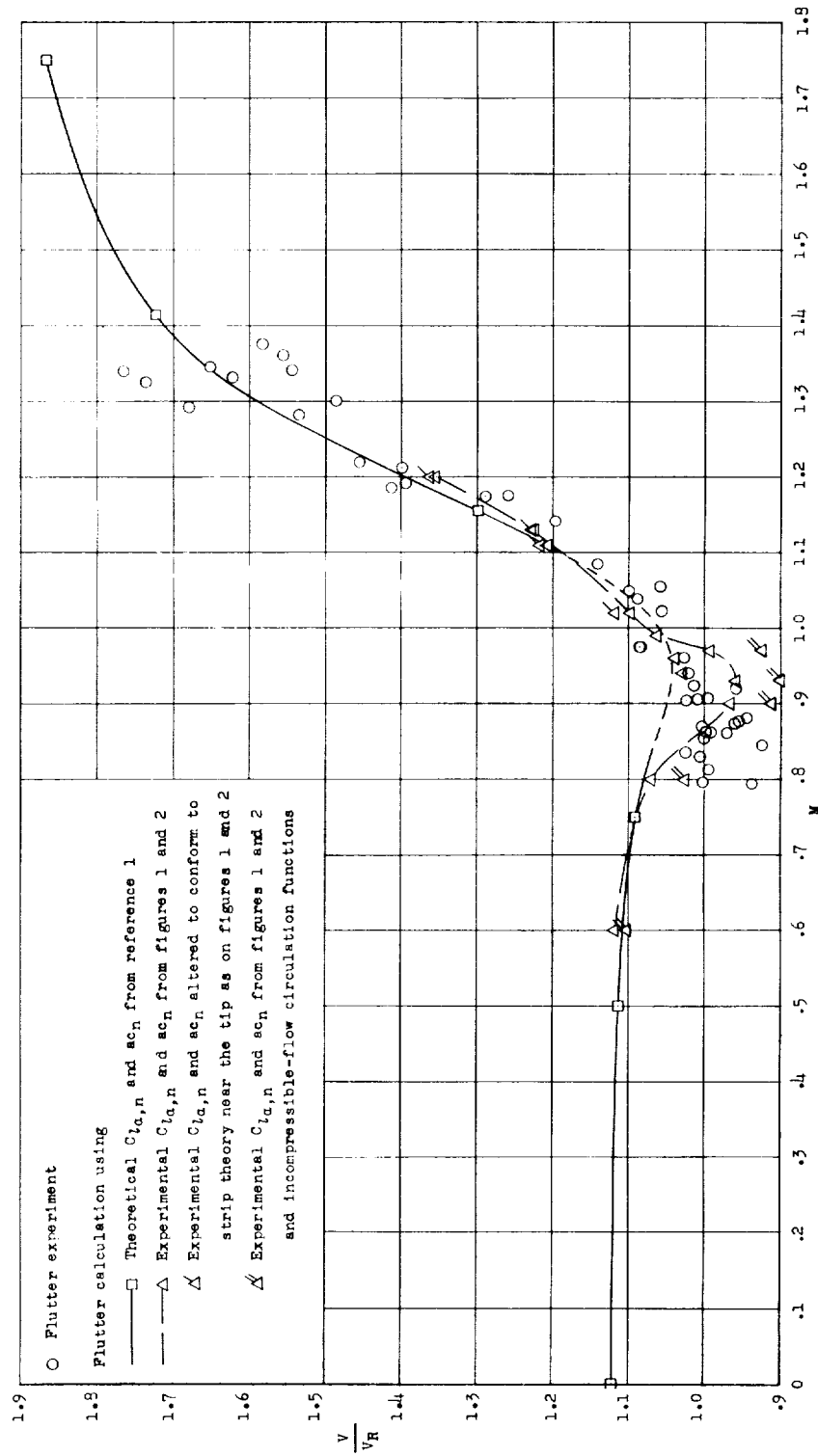


Figure 10.- Variation of flutter speed with Mach number for wing 445. For calculated points $\rho = 0.003800$ slug/cu ft and $V_R = 735.0$ ft/sec.

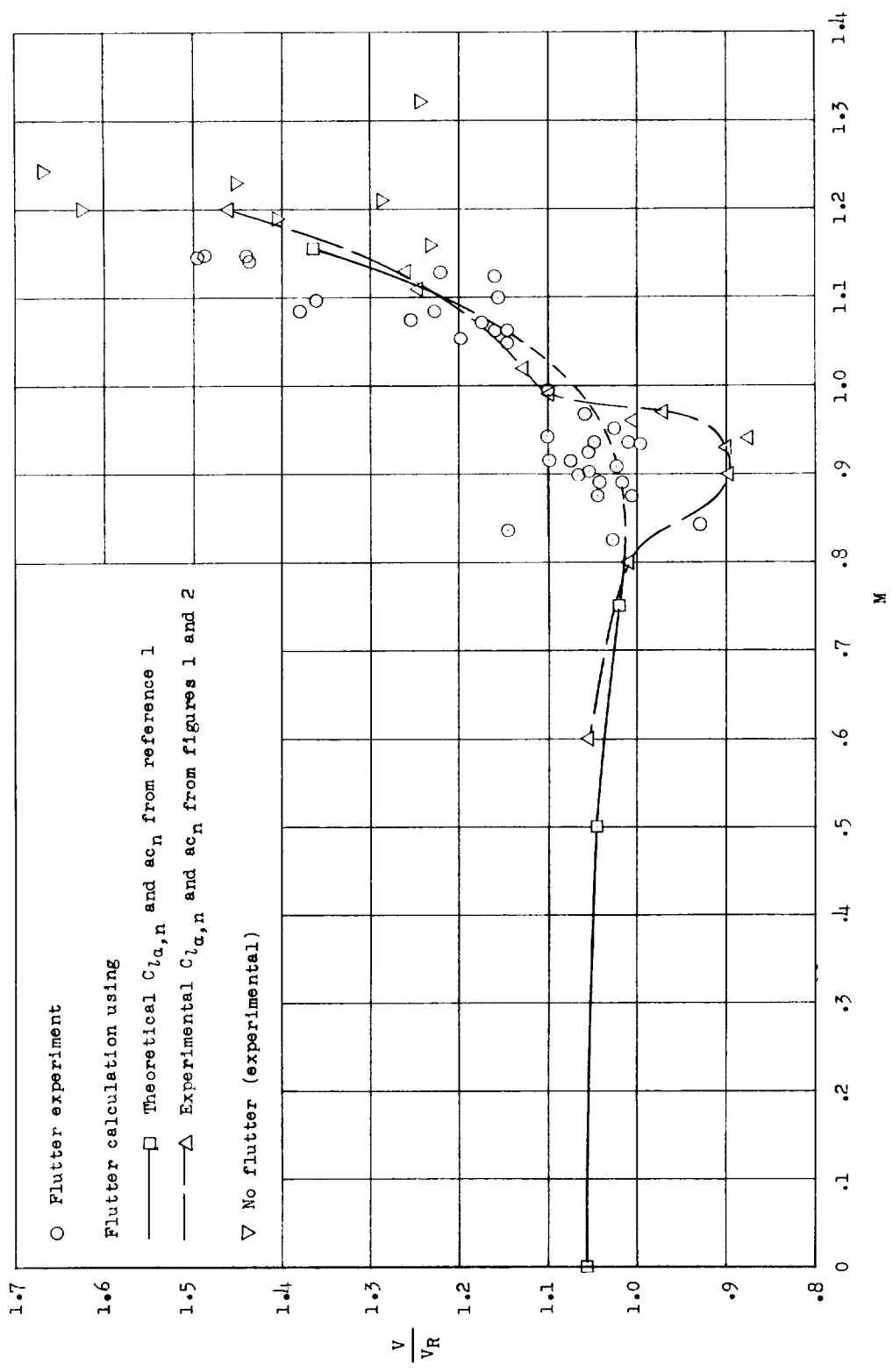


Figure 11.- Variation of flutter speed with Mach number for wing 445F. For calculated points $\rho = 0.003000$ slug/cu ft and $V_R = 840.0$ ft/sec.

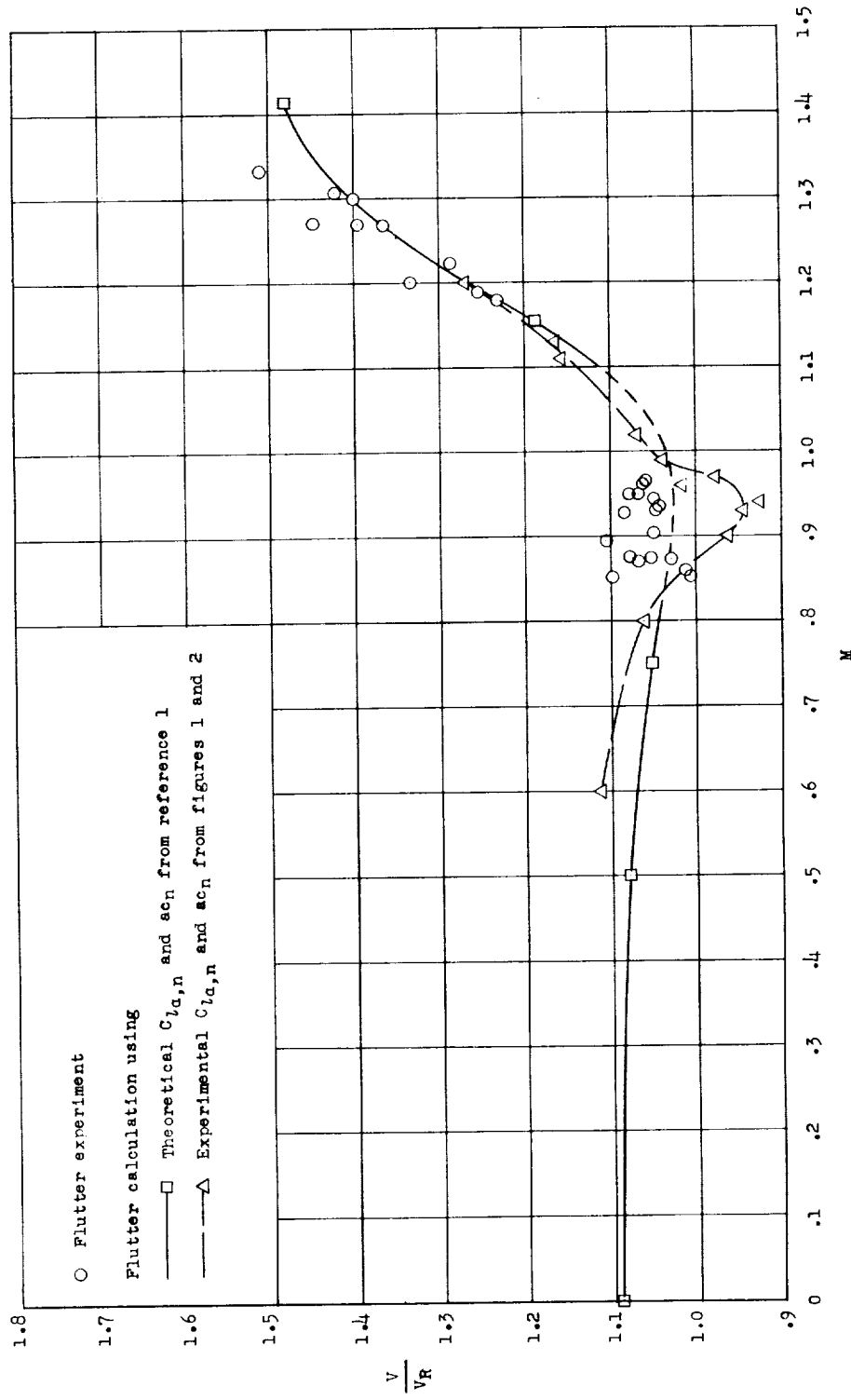


Figure 12.- Variation of flutter speed with Mach number for wing 445R. For calculated points $\rho = 0.002378$ slug/cu ft and $V_R = 928.7$ ft/sec.

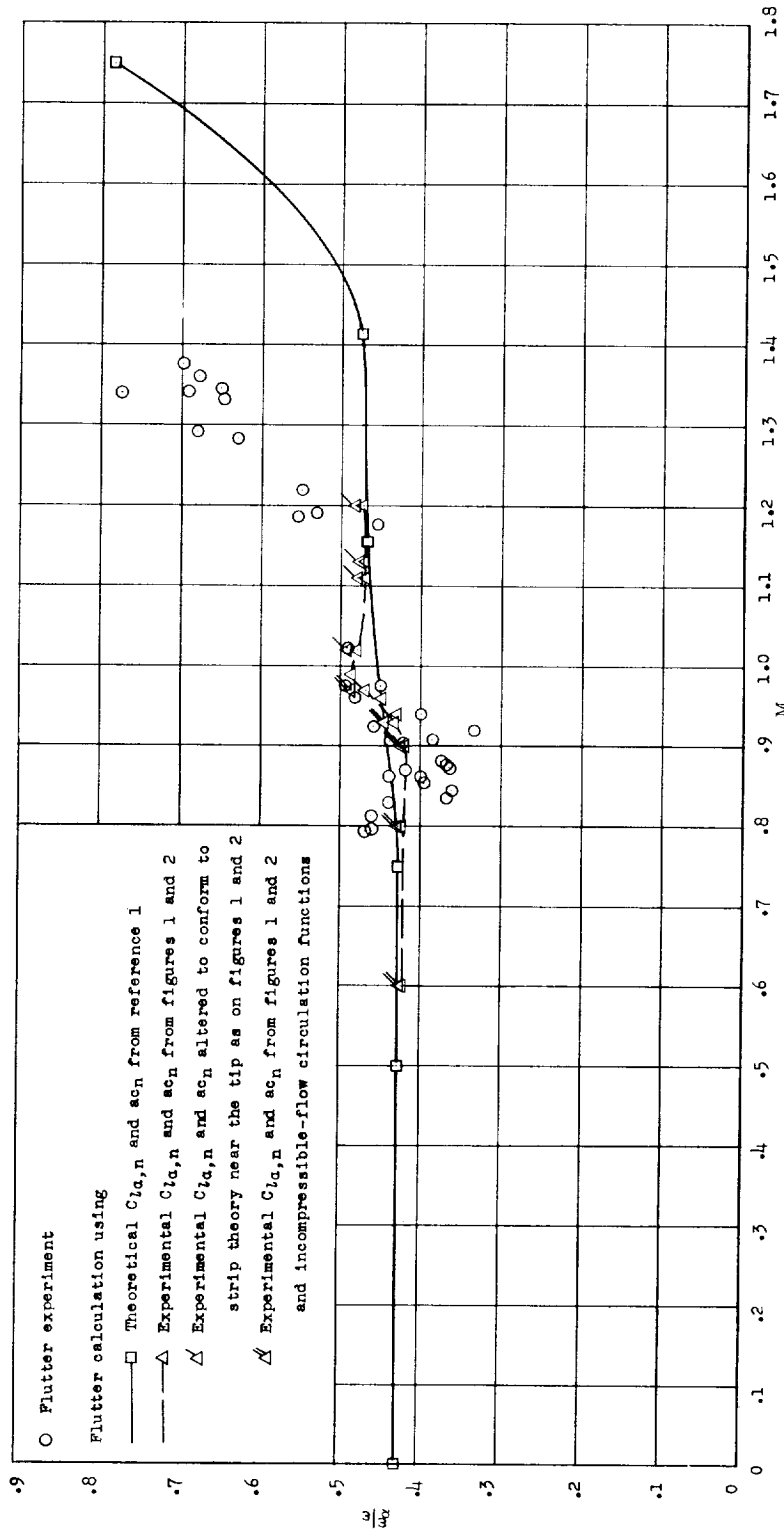


Figure 13.- Variation of flutter frequency with Mach number for wing 445. For calculated points $\rho = 0.003800$ slug/cu ft and $\omega_{\alpha} = 2,192$ radians/sec.

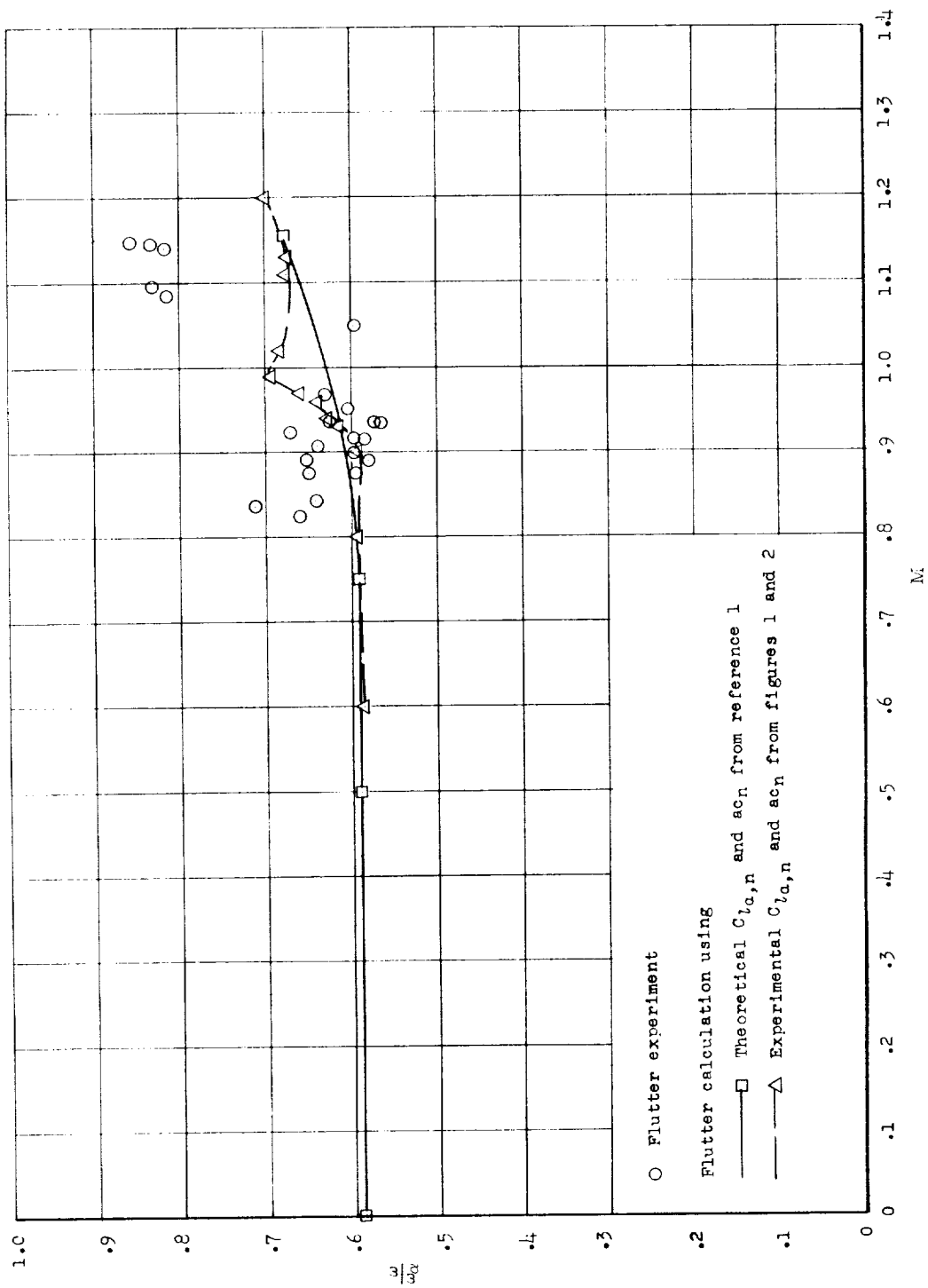


Figure 14.- Variation of flutter frequency with Mach number for wing 445F. For calculated points $\rho = 0.003000$ slug/cu ft and $\omega_b = 1,144$ radians/sec.

CONFIDENTIAL

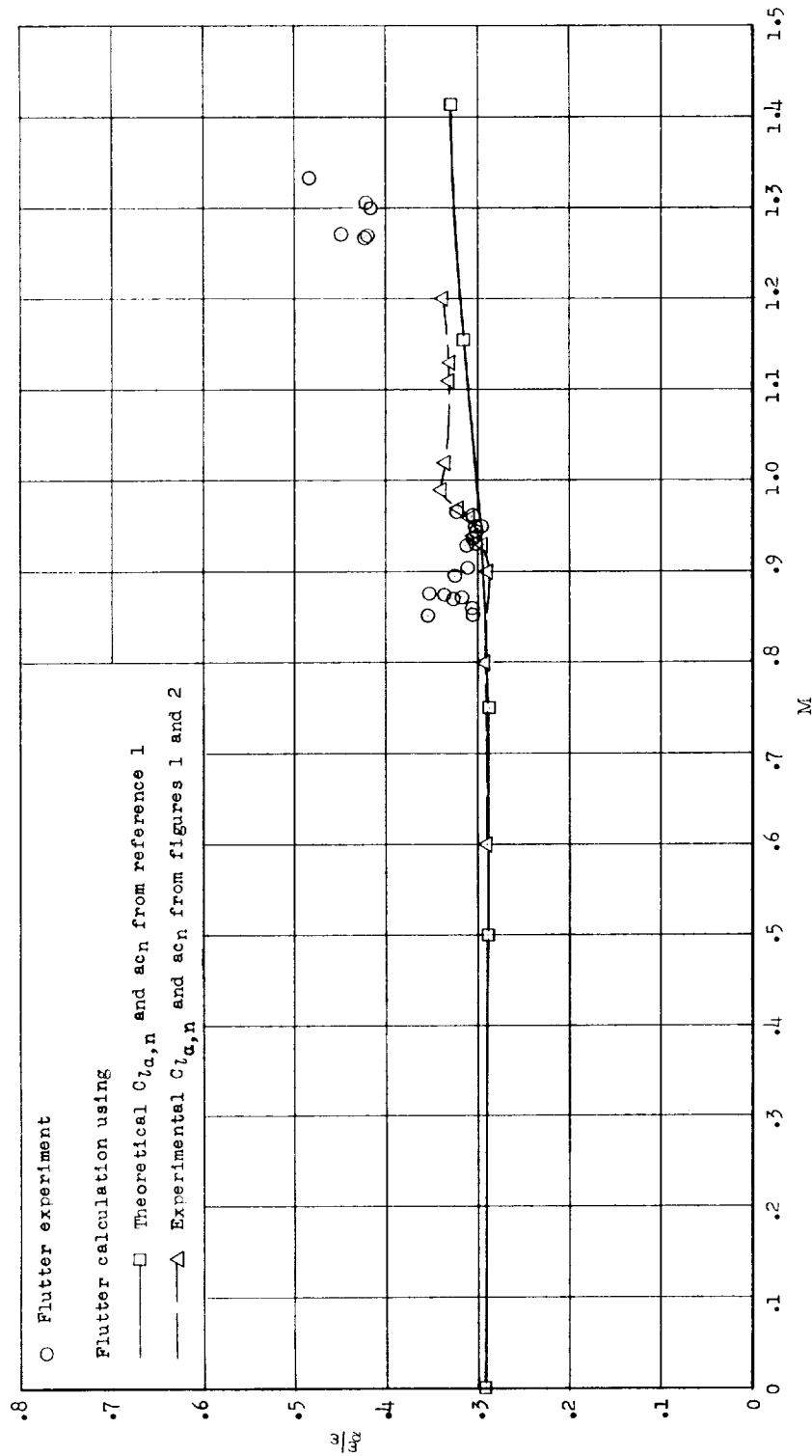


Figure 15.- Variation of flutter frequency with Mach number for wing 445R. For calculated points $\rho = 0.002378$ slug/cu ft and $\omega_a = 2,306$ radians/sec.

CONFIDENTIAL

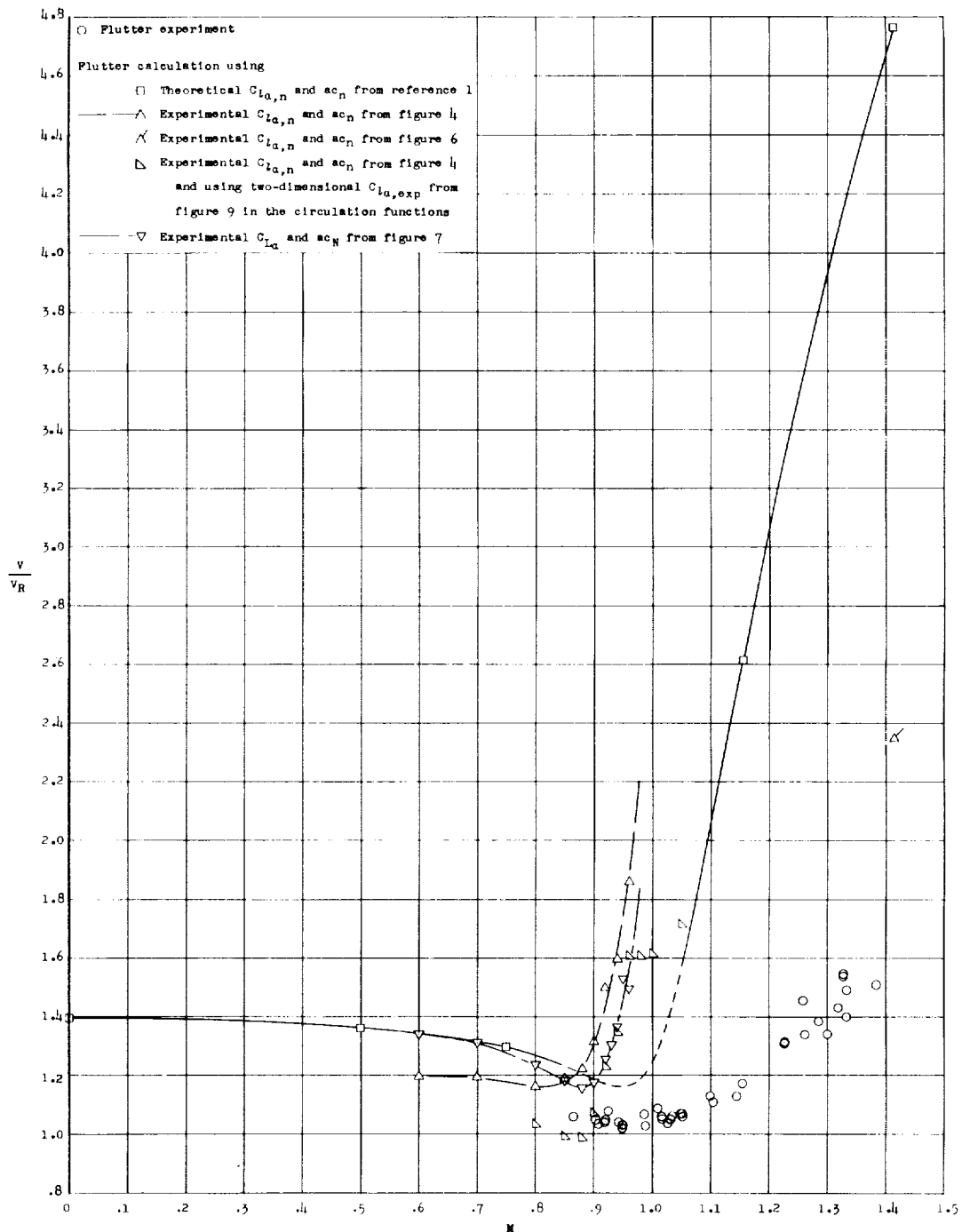


Figure 16.- Variation of flutter speed with Mach number for wing 400. For calculated points $\rho = 0.002378$ slug/cu ft and $V_R = 976.5$ ft/sec.

CONFIDENTIAL

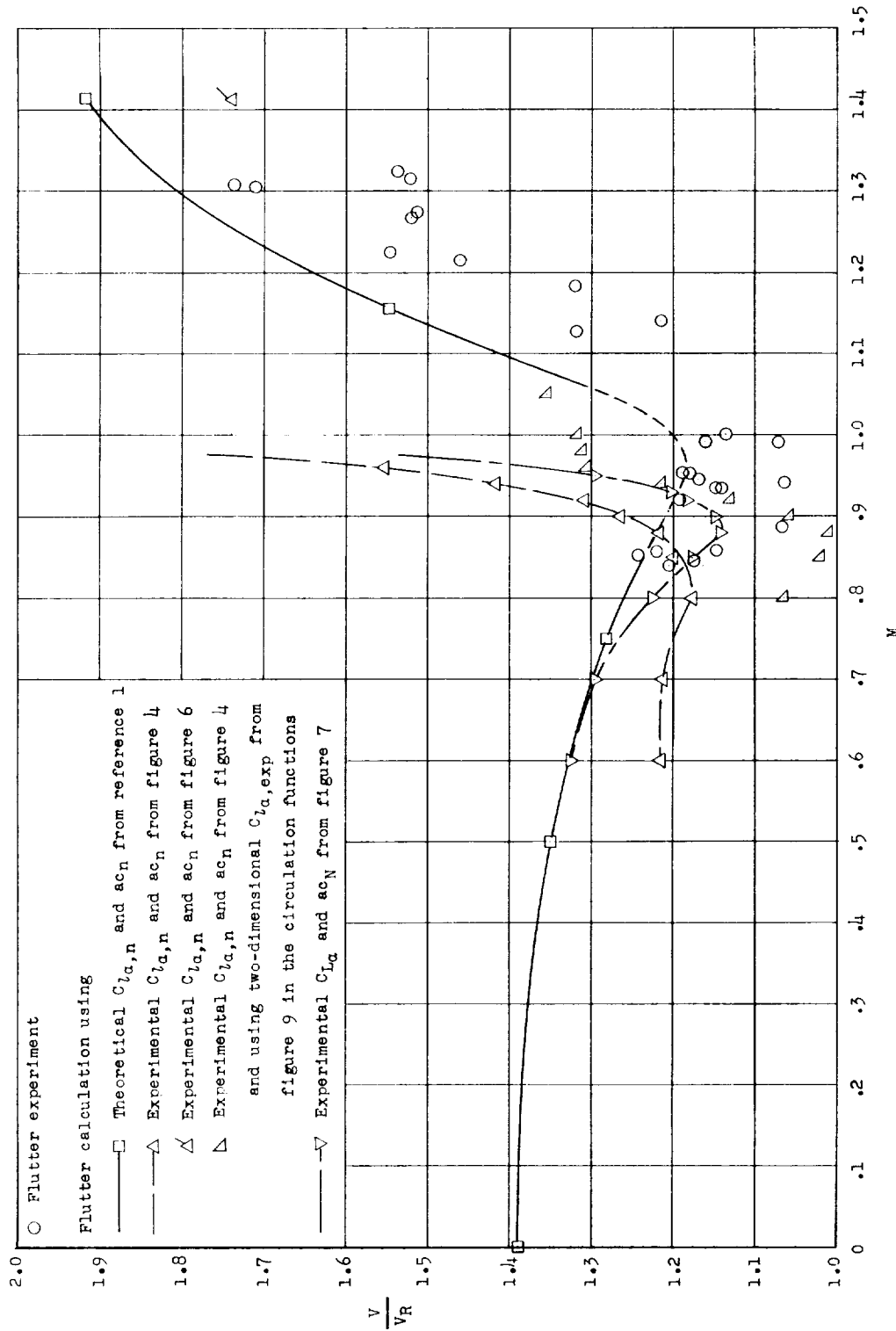


Figure 17.- Variation of flutter speed with Mach number for wing 400R. For calculated points $\rho = 0.003100$ slug/cu ft and $V_R = 852.5$ ft/sec.

CONFIDENTIAL

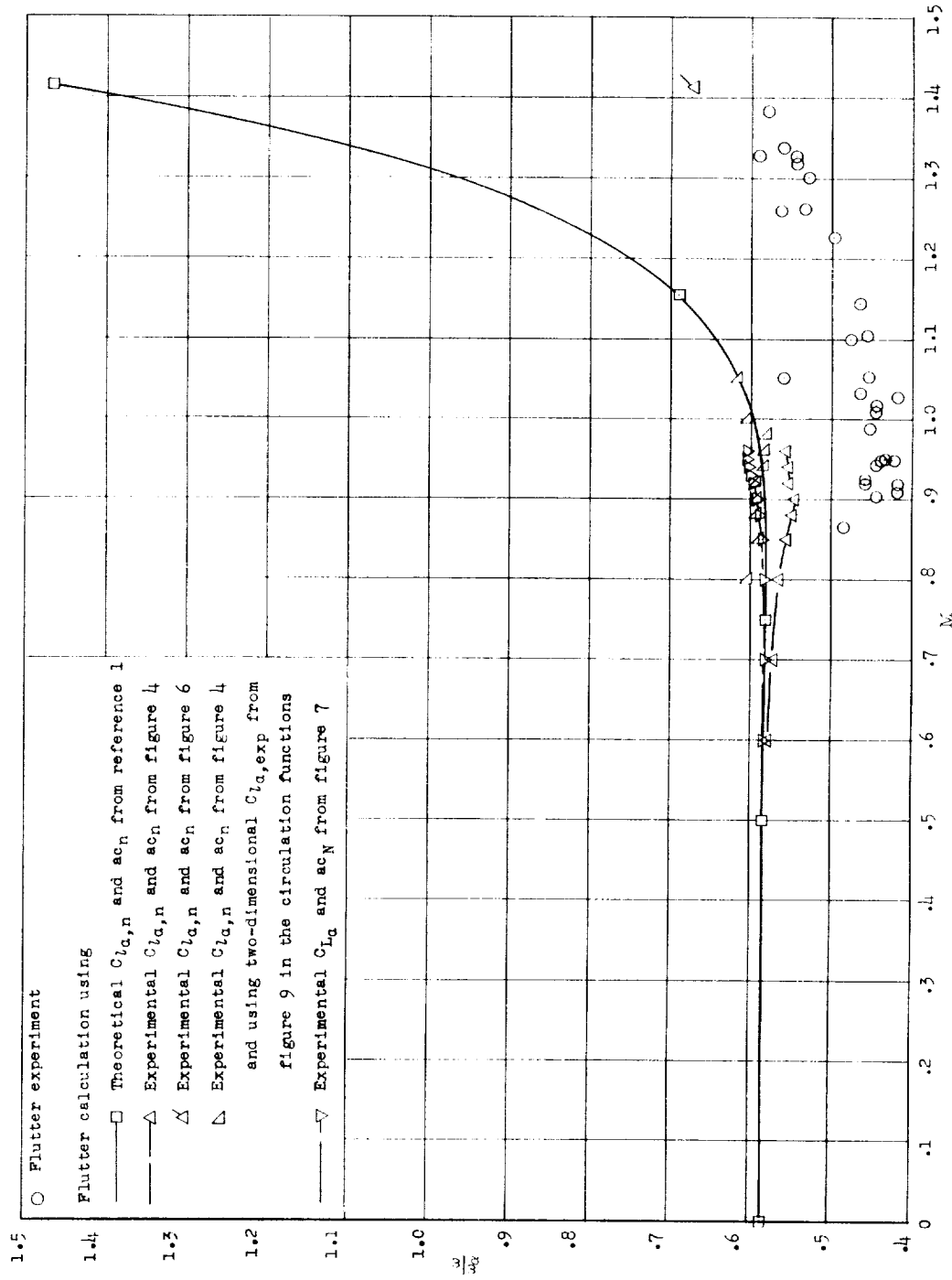


Figure 18.- Variation of flutter frequency with Mach number for wing 400. For calculated points $\rho = 0.002378$ slug/cu ft and $\omega_q = 2,463$ radians/sec.

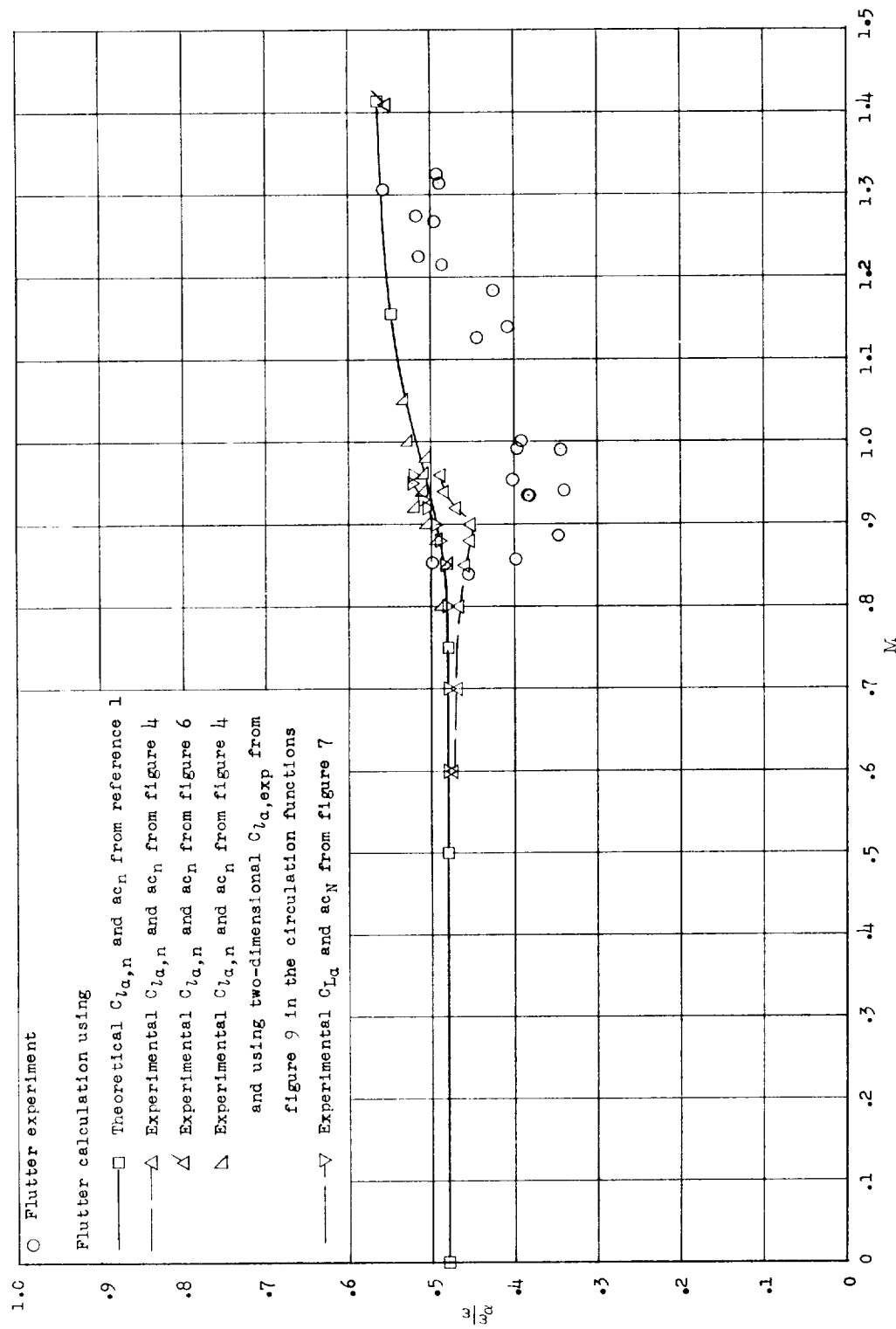


Figure 19.- Variation of flutter frequency with Mach number for wing 400R. For calculated points $\rho = 0.003100$ slug/cu ft and $\omega_\alpha = 1,982$ radians/sec.

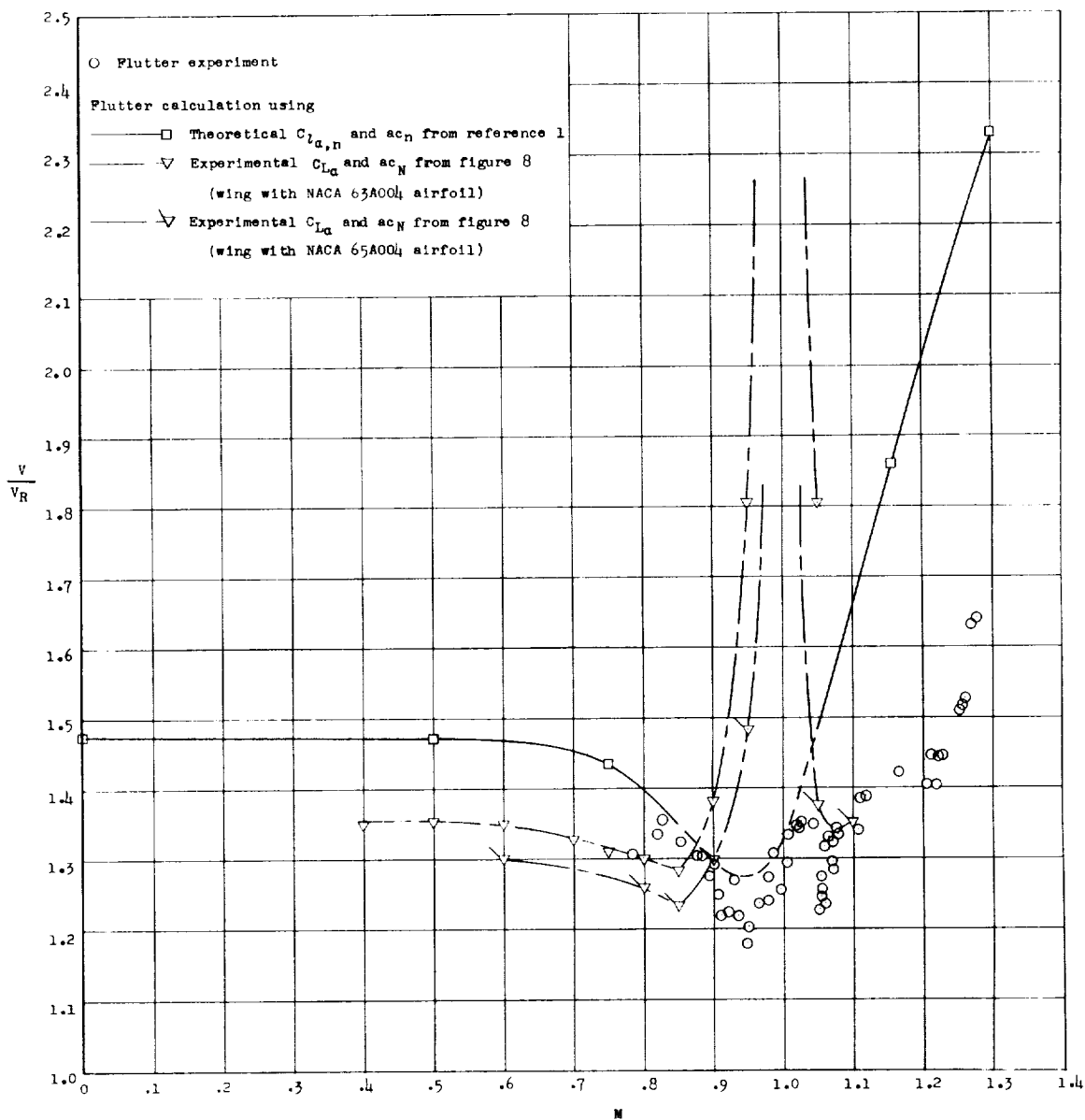


Figure 20.- Variation of flutter speed with Mach number for wing 4001. For calculated points $\rho = 0.002378$ slug/cu ft and $V_R = 828.5$ ft/sec.

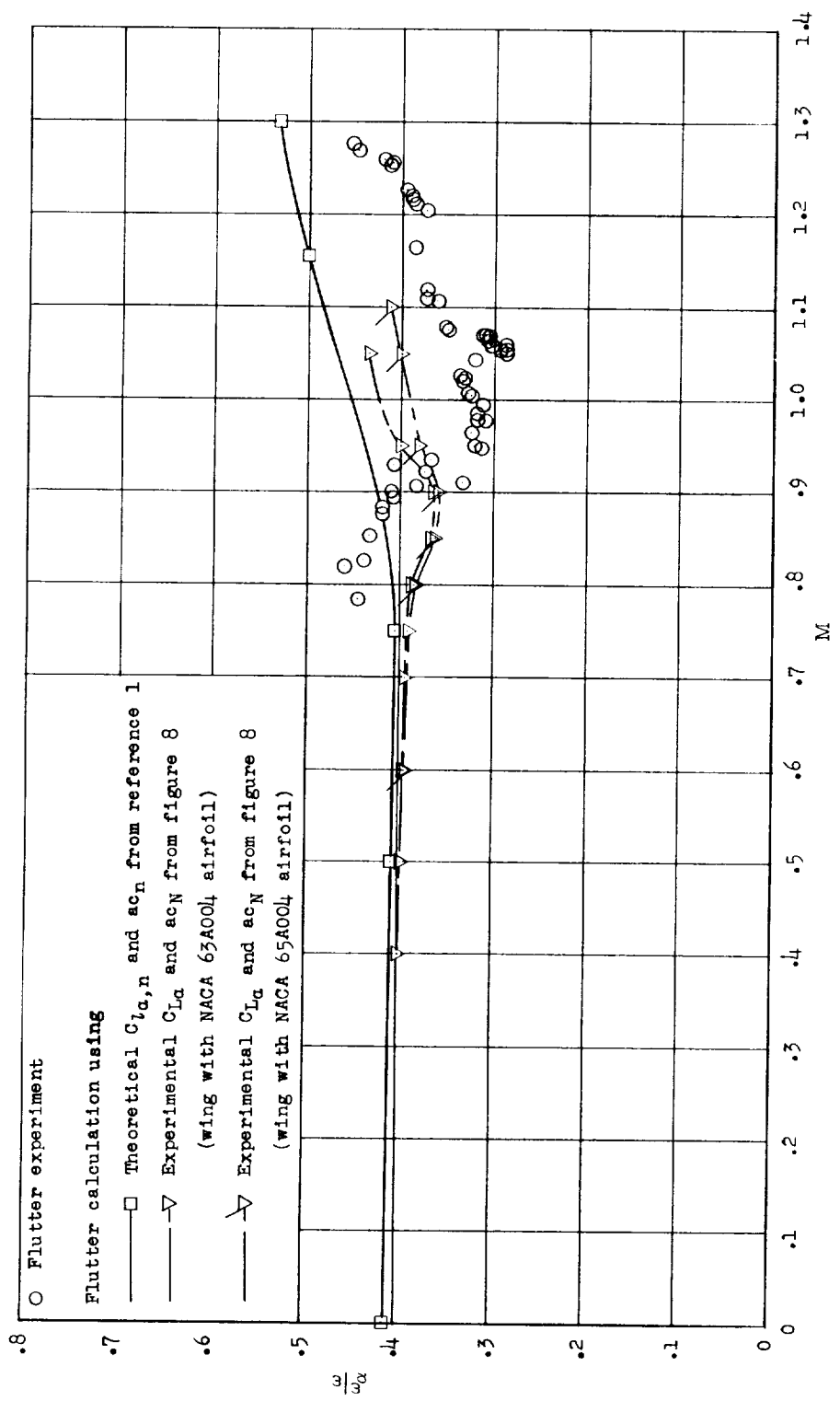


Figure 21.- Variation of flutter frequency with Mach number for wing 4001. For calculated points $\rho = 0.002378$ slug/cu ft and $\omega\alpha = 2,048$ radians/sec.

THE FUTURE OF THE FUTURE

03141950 1040

CONFIDENTIAL

CONFIDENTIAL
DECLASSIFIED